NAVAL POSTGRADUATE SCHOOL

MONTEREY, CALIFORNIA

THESIS

DIRECT-CONNECT PERFORMANCE EVALUATION OF A VALVELESS PULSE DETONATION ENGINE

by

Nicole Kay Wittmers

December 2004

Thesis Advisor:	Christopher Brophy
Second Reader:	Garth Hobson

Approved for public release; distribution is unlimited.

THIS PAGE INTENTIONALLY LEFT BLANK

REPORT DOCUMENTATION PAGE			Form Approved OMB No. 0704-0188
Public reporting burden for this collection of information is estimated to average 1 hour per response, including the time for reviewing instruction, searching existing data sources, gathering and maintaining the data needed, and completing and reviewing the collection of information. Send comments regarding this burden estimate or any other aspect of this collection of information, including suggestions for reducing this burden, to Washington headquarters Services, Directorate for Information Operations and Reports, 1215 Jefferson Davis Highway, Suite 1204, Arlington, VA 22202-4302, and to the Office of Management and Budget, Paperwork Reduction Project (0704-0188) Washington DC 20503.			
1. AGENCY USE ONLY *(Leave blank)*	**2. REPORT DATE** December 2004	**3. REPORT TYPE AND DATES COVERED** Master's Thesis	
4. TITLE AND SUBTITLE: Direct-Connect Performance Evaluation of a Valveless Pulse Detonation Engine			**5. FUNDING NUMBERS N00014OWR20226**
6. AUTHOR(S) Nicole Wittmers			
7. PERFORMING ORGANIZATION NAME(S) AND ADDRESS(ES) Naval Postgraduate School Monterey, CA 93943-5000			**8. PERFORMING ORGANIZATION REPORT NUMBER**
9. SPONSORING /MONITORING AGENCY NAME(S) AND ADDRESS(ES) Office of Naval Research Ballston Tower One 800 N. Quincy Street Arlinton, VA 22217-5660			**10. SPONSORING/MONITORING AGENCY REPORT NUMBER**
11. SUPPLEMENTARY NOTES The views expressed in this thesis are those of the author and do not reflect the official policy or position of the Department of Defense or the U.S. Government.			
12a. DISTRIBUTION / AVAILABILITY STATEMENT Approved for public release; distribution unlimited.			**12b. DISTRIBUTION CODE**

13. ABSTRACT

Operational characteristics of a valveless pulse detonation engine system were characterized by experimental measurements of thrust, fuel flow, and internal gas dynamics. The multi-cycle detonation experiments were performed on an axis-symmetric engine geometry operating on an ethylene/air mixtures. The detonation diffraction process from a small 'initiator' combustor to a larger diameter main combustor in a continuous airflow configuration was evaluated during multi-cycle operation of a pulse detonation engine and was found to be very successful at initiating combustion of the secondary fuel/air mixture at high frequencies. The configuration was used to demonstrate the benefit of generating an overdriven detonation condition near the diffraction plane for enhanced transmission of the larger combustor. Results have shown that the addition of optical sensors, such as tunable diode lasers, to provide fuel profile data are invaluable for providing high fidelity performance results. The performance results demonstrated the ability of the valveless pulse detonation engine to run at efficiencies similar to valved pulse detonation engine geometries and may be a low cost alternative to conventional air-breathing propulsion systems.

14. SUBJECT TERMS Pulse Detonation Engine, Supersonic Air Breathing, Engine Performance Evaluation			**15. NUMBER OF PAGES** 79
			16. PRICE CODE
17. SECURITY CLASSIFICATION OF REPORT Unclassified	**18. SECURITY CLASSIFICATION OF THIS PAGE** Unclassified	**19. SECURITY CLASSIFICATION OF ABSTRACT** Unclassified	**20. LIMITATION OF ABSTRACT** UL

NSN 7540-01-280-5500

Standard Form 298 (Rev. 2-89)
Prescribed by ANSI Std. 239-18

THIS PAGE INTENTIONALLY LEFT BLANK

Approved for public release; distribution is unlimited.

DIRECT-CONNECT PERFORMANCE EVALUATION OF A VALVELESS PULSE DETONATION ENGINE

Nicole K.Wittmers
Lieutenant , United States Navy
B.S., United States Naval Academy, 1999

Submitted in partial fulfillment of the
requirements for the degree of

MASTER OF SCIENCE IN ASTRONAUTICAL ENGINEERING

from the

NAVAL POSTGRADUATE SCHOOL
December 2004

Author: Nicole K. Wittmers

Approved by: Christopher M. Brophy
Thesis Advisor

Garth Hobson
Second Reader/Co-Advisor

Anthony Healey
Chairman, Department of Mechanical & Astronautical Engineering

THIS PAGE INTENTIONALLY LEFT BLANK

ABSTRACT

Operational characteristics of a valveless pulse detonation engine system were characterized by experimental measurements of thrust, fuel flow, and internal gas dynamics. The multi-cycle detonation experiments were performed on an axis-symmetric engine geometry operating on an ethylene/air mixtures. The detonation diffraction process from a small 'initiator' combustor to a larger diameter main combustor in a continuous airflow configuration was evaluated during multi-cycle operation of a pulse detonation engine and was found to be very successful at initiating combustion of the secondary fuel/air mixture at high frequencies. The configuration was used to demonstrate the benefit of generating an overdriven detonation condition near the diffraction plane for enhanced transmission of the larger combustor. Results have shown that the addition of optical sensors, such as tunable diode lasers, to provide fuel profile data are invaluable for providing high fidelity performance results. The performance results demonstrated the ability of the valveless pulse detonation engine to run at efficiencies similar to valved pulse detonation engine geometries and may be a low cost alternative to conventional air-breathing propulsion systems.

THIS PAGE INTENTIONALLY LEFT BLANK

TABLE OF CONTENTS

THIS PAGE INTENTIONALLY LEFT BLANK

LIST OF FIGURES

THIS PAGE INTENTIONALLY LEFT BLANK

LIST OF TABLES

THIS PAGE INTENTIONALLY LEFT BLANK

ACKNOWLEDGMENTS

The author would like to acknowledge the financial support of the Office of Naval Research under ONR Contract N00014OWR20226.

The author would also like to thanks Professor Christopher Brophy, Professor Jose Sinibaldi, and Professor Garth Hobson for the invaluable assistance and education provided me during the development of this thesis. The completion of this work would not have been possible without them.

The author would like to thank Mr. George Hageman for his extensive work on the testing equipment and test cell development for this thesis. His hard work and dedication directly contributed to the author being able to graduate on time.

In addition, Mr. Frank Franzen and Mr. James Lefler need to be thanked for their outstanding machining of the Pulse Detonation Engine components used in this thesis.

THIS PAGE INTENTIONALLY LEFT BLANK

LIST OF SYMBOLS AND ABREVIATIONS

A	Area
C_p	Constant Pressure Specific Heat
C-J	Chapman Jouget Point
c	Local Sonic Velocity
e	Total Internal Energy per Unit Mass
h	Enthalpy per Unit Mass
h°	Enthalpy of Formation
M	Mach Number
$\dot{m}$	Mass Flow Rate
p	Pressure
p_o	Ambient Pressure
q	Total Heat Addition per Unit Mass
q_{cond}	Heat Addition per Unit Mass by Conduction
$q_{addition}$	Heat Addition by Combustion
$q_{1\text{-}2}$	Heat Addition by Combustion
$q_{0\text{-}4}$	Heat Released into Atmosphere
R	Specific Gas Constant
s	Entropy
T	Temperature
u	Velocity
u’	Internal Energy
V_{det}	Detonation Velocity
W_{net}	Net Work
x	Position
γ	Specific Heat Ratio
λ_c	Thermal Conductivity
λ	Cell Size
η_{TH}	Thermal Effieciency
ϕ	Equivalence Ratio
ρ	Density
ν	Specific Volume ($\frac{1}{\rho}$)
I_{sp}	Specific Impulse

THIS PAGE INTENTIONALLY LEFT BLANK

I. INTRODUCTION

A. BACKGROUND

This investigation was conducted as part of the Office of Naval Research program for fundamental research into pulse detonation engines (PDEs). The study involved the installation and calibration of a six degree-of-freedom (DOF) thrust stand awarded to Naval Postgraduate School (NPS), for the performance characterization of the NPS PDE geometry. The performance testing capabilities of the new test stand provide high fidelity benchmark data for system modelers and other researchers in the PDE area.

Over the past 10 years, pulse detonation engines have received a considerable amount of interest due to their potential for increased specific impulse values on a low cost engine architecture when compared to existing supersonic engine systems. These engines operate by producing detonation waves that propagate through a premixed fuel/air mixture and produce intermittent high chamber pressures which result in discrete impulses that may be averaged to produce a quasi-steady thrust [1]. The concept of using detonations as a means for propulsion is based on the simple concept of using a thrust tube, with a closed head end and an open downstream end, in which detonation waves are produced in a repetitive manner. A fuel/air mixture is injected at the beginning of each cycle, ignited, and the resulting deflagration wave quickly transitions into a detonation wave. This produces significant head-end pressure at the closed end and ultimately thrust by the exiting momentum flux. After the detonation wave exits the combustor, an expansion wave (rarefraction wave) travels from the exit of the combustor to the head wall relieving the high pressure and removing the hot combustion products from the combustor. Although most PDE systems evaluated in the past have utilized valved geometries, the valveless geometry being explored at NPS is an alternative architecture which could greatly reduce complexity and cost.

B. PREVIOUS RESEARCH

Previous studies at the NPS have explored the use of ethylene/air, propane/air, and JP10/air mixtures on the NPS valveless pulse detonation engine. Ethylene was chosen due to its increased detonation sensitivity and propane for its combustion

similarities to higher-order hydrocarbon fuels. Practical operation of these systems ultimately requires the use of fuels that have acceptance or approval by the military, such as JP-10. The use of such fuels has inherent difficulties since most fuel/air mixtures are often difficult to detonate [2], especially in a reliable and repetitive manner. Therefore, an initiator which consists of a small tube or auxiliary combustor filled with a highly detonable fuel/oxygen mixture is often used as a means to initiate a detonation in a larger main combustor containing a less sensitive fuel/air mixture [2].

The use of an initiator has proven reliable in ensure the detonation of the fuel/air mixture in the main combustor, but it does introduce a penalty on the performance of the system [3]. This highly detonable fuel/oxygen mixture is used due to its ability to provide reliable, repeatable, and very rapid ignition events. The volume and mass requirement to carry an auxiliary oxygen delivery system results in a loss in performance. This is due to the fact that it is treated as a 'fuel' for specific impulse (I_{sp}) calculations. As shown in equation (1), the I_{sp} is a relationship of the mass of the fuel used and the force that is created by the system.

$$I_{sp_f} = \frac{F_{NET}}{m_{fuel} g} = \frac{F_{NET}}{(m_{fuel} + m_{O_2\,Aux}) g} \tag{1}$$

Therefore, the less oxygen that is added to the system the better the performance delivered by the overall system. Equation (1) shows the direct relation on how advantageous it would be to create a system that would work without the need for auxiliary oxygen in the system.

II. DETONATION THEORY

A. DETONATIONS, DEFLAGRATIONS, AND EXPLOSIONS

The difference between a detonation and other combustion events is significant enough to require clarification to fully understand the pulse detonation engine cycle. The differences between detonations, deflagrations, and explosions can be understood by first discussing what the combustion process involves.

Combustion is defined as an exothermic chemical reaction between a fuel and an oxidizer that once initiated can sustain itself as long as those ingredients are available in the proper proportions. The velocity at which the combustion wave propagates through the mixture is a relative measure of the strength of the event. The geometry of the volume, mixture composition, temperature, mixture conditions (i.e. turbulence levels), and pressure are all factors on which the combustion flame velocity is dependent.

There are primarily three types of combustion process: a) Deflagration, where a combustion wave propagates at subsonic speed and there is little or no pressure change across the flame front, b) Detonation, where a combustion wave propagates at supersonic speed with a substantial pressure rise across the flame front, and c) Explosion, where the rate of heat generation is extremely fast, but it does not require the passage of a combustion wave through the exploding medium. The detonation process has the lowest entropy rise for the given energy release relative to the deflagration process, producing more work available for propulsion means and an overall higher thermodynamic efficiency. [4]

Deflagration is a combustion wave that propagates slower than the speed of sound (subsonic) into unburned reactants. Examples of the deflagration processes include the combustion of a simple birthday candle to the flame within a gas turbine engine. The flame speed is a function of pressure, temperature, mixture ratio and turbulence of reactants. The typical wave speeds for a deflagration will range from 1-30 m/s. This is not the most efficient thermodynamic path for combustion to occur. This is due to the fact that the entropy of the resulting gases is maximized which results in a reduced about of work available for subsequent thermodynamic processes. [4]

A detonation can be described as a supersonic combustion event that propagates at high velocities into a detonable mixture and produces a violent and rapid combustion of reactants due to the strong shock wave leading the combustion wave. The propagation characteristics of these waves are primarily a function of fuel-to-oxidizer ratio (equivalence ratios) and have specific velocities, pressures rises, and temperature ratios that are limited by thermodynamic considerations.

A detonation wave can be modeled as a one-dimensional stationary plane wave, as seen in Figure 1. As the reactants "pass through" the combustion wave from right to left, the ratio of the product properties to the reactant properties depends on whether the planar wave is a detonation or a deflagration. Table 1 shows the comparison of properties between deflagration and detonation events. These allow for an easy determination of which type of combustion process has occurred.

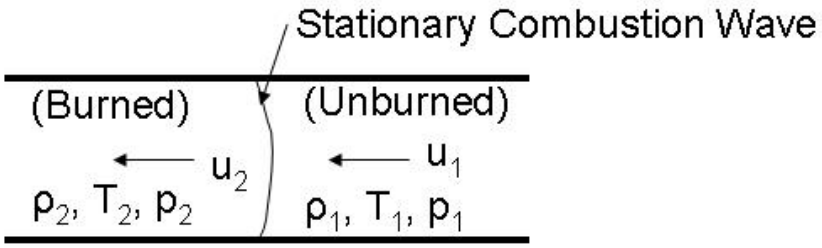

Figure 1. Stationary Combustion Wave

Properties	Deflagration	Detonation
u_1/c_1	0.0001 - 0.03	5 – 10
u_2/u_1	4 - 6 (acceleration)	0.4 - 0.7 (deceleration)
p_2/p_1	≅ 0.98 (slight expansion)	13 - 55 (compression)
T_2/T_1	4 - 16 (heat addition)	8 - 21 (heat addition)
ρ_2/ρ_1	0.06 - 0.25	1.7 - 2.6

Table 1. Differences between Detonation and Deflagration from Ref [2]

In an explosion, a chemical exothermic reaction occurs at a rate much greater than the surrounding environment can absorb or dissipate. This reaction rate will increase exponentially with a subsequent increase in temperature and pressure resulting in the combustion event to drive itself out of control quickly. The volume of the explosion will

expand due to massive increase in pressure which forms a supersonic shock front. Though an explosion is powerful and occurs at a rapid rate, the combustion even itself is a deflagration wave. [3]

B. THE RANKINE-HUGONOIT CURVE

To understand the properties of a detonation wave, it is helpful to begin with an analysis of the Rankine-Hugoniot curve. This curve shows the relationship between enthalpy, pressure, and the density of gases in a combustion event. The process is assumed to take place in a constant area geometry.

The Rankine-Hugoniot relation is generated by using three consecutive equations which determine the post-combustion state thermodynamic properties:

Continuity :
$$\frac{d(\rho u)}{dx} = 0 \tag{2}$$

Conservation of momentum:
$$\rho u \frac{du}{dx} = -\frac{dp}{dx} \tag{3}$$

Conservation of energy:

$$\rho u \left[\frac{d}{dx}\left(h + \frac{u^2}{2} \right) \right] = -\frac{d}{dx}(q_{cond}) \tag{4}$$

Enthalpy and the heat added to the system are defined by the following system of equations.

$$h = C_p T + h^{\circ} \tag{5}$$

$$q = h_1^{\circ} - h_2^{\circ} \tag{6}$$

$$q_{cond} = -\lambda \frac{dT}{dx} \tag{7}$$

This derivation assumes steady one-dimensional flow with no external heat added or rejected from the system. The diffusion effects and viscous effects are assumed to be negligible as well. By making these assumptions, the detonation wave can be viewed as a supersonic shock wave with calculable properties both in front and behind the wave. By integrating equation (2) the requirement of constant mass flow rate can be stated.

$$\int d(\rho u) = \int 0 dx \Rightarrow \rho u A = const = \dot{m} \tag{8}$$

Now, by substitution the equation for mass flow rate into the momentum equation (3) and simplifying,

$$\frac{d}{dx}\left[\rho u^2 + p\right] = 0 \tag{9}$$

Integrating this equation gives an alternate momentum equation.

$$\rho u^2 + p = const' \tag{10}$$

By similar analysis, the energy equation becomes:

$$\rho u\left(C_p T + h^\circ + \frac{u^2}{2}\right) - \lambda_c \frac{dT}{dx} = const'' \tag{11}$$

Referring back to Figure 1. and knowing that the change in temperature with respect to the position (dT/dx) in front of and behind the detonation wave is equal to zero, specific conservation equations can be derived. These equations relate the fluid dynamic and thermodynamic properties between the two regions. These equations are:

$$\rho_1 u_1 = \rho_2 u_2 = const. = \dot{m} \tag{12}$$

$$p_1 + \rho_1 u_1^{\,2} = p_2 + \rho_2 u_2^{\,2} \tag{13}$$

$$C_p T_1 + \frac{1}{2}u_1^2 + q = C_p T_2 + \frac{1}{2}u_2^2 \tag{14}$$

Combining equations (5), (6), and (13) results in

$$h_1 + \frac{u_1^2}{2} + q = h_2 + \frac{u_2^2}{2} \tag{15}$$

The final equation needed for deriving the Rankine-Hugoniot relation is found by the assumption that the gases in both the burned and unburned regions behave like a perfect gas, therefore

$$p = \rho RT \tag{16}$$

Equations (12), (13), (15),and (16) are the set of equations used to solve the five unknowns of the system, u_1,u_2,T_2, p_2, and ρ_2. One equation with two unknowns (p_2 and ρ_2) can be formed by manipulated the four basic equations with the following outcome:

$$\rho_1^2 u_1^2 = \frac{p_2 - p_1}{\frac{1}{\rho_1} - \frac{1}{\rho_2}} = \dot{m}^2 \tag{17}$$

Equation (17) is the Rayleigh line equation, which describes the heat addition process through pressure, velocity, and density. It is more useful to describe the characteristics of thermodynamics in terms of the flow Mach number. This is completed by the following:

$$M = \frac{u}{c} \tag{18}$$

$$c = \sqrt{\gamma RT} \tag{19}$$

Manipulating and substituting the equations can result in the following:

$$\frac{\gamma}{\gamma}\frac{\rho_1^2 u_1^2}{\rho_2^2 u_2^2} = \frac{\frac{p_2}{p_1} - 1}{1 - \frac{\rho_1}{\rho_2}} = \gamma M_1^2 \tag{20}$$

Knowing that,

$$C_p - C_v = R \Rightarrow C_p = \left(\frac{\gamma}{\gamma - 1}\right) R \tag{21}$$

Equation (14) can now be rewritten as:

$$\left(\frac{\gamma}{\gamma-1}\right)\left(\frac{p_2}{\rho_2}-\frac{p_1}{\rho_1}\right)-\left(\frac{1}{2}\right)(p_2-p_1)\left(\frac{1}{\rho_2}+\frac{1}{\rho_1}\right)=q \tag{22}$$

and

$$h_2-h_1=\frac{1}{2}(p_2-p_1)(\frac{1}{\rho_1}+\frac{1}{\rho_2}) \tag{23}$$

Equations (22) and (23) are forms of the Rankine-Hugoniot relation. [2]

The Rankine-Hugoniot curve is a plot that describes the different possible thermodynamic conditions after combustion occurs. These conditions include various strengths of deflagrations and detonations, dependent upon the specific volume and pressure at which the event occurs. Figure 2. shows the Rankine-Hugoniot curve and the various combustion regions. Regions I through V are all regions of possible mathematical solutions. In reality, not all of the regions are physically realizable. For example, region V implies that the initial internal energy is imaginary. Careful analysis of the Rankine-Hugoniot curve shows that there are two possible combustion processes: those in which pressure and density increase (detonations) and those in which pressure and density decrease (deflagrations). The points at which the Rankine-Hugoniot curve and the Rayleigh lines are tangent are known as the upper(U) and lower (L) Chapman-Jouguet points. These points represent where the post combustion gas velocity is sonic, as dictated by the Rayleigh limit for heat addition in a constant area tube. Table 2 depicts the type of combustion process and the Mach numbers of the reactants and products in each region of the Rankine-Hugonoit curve.

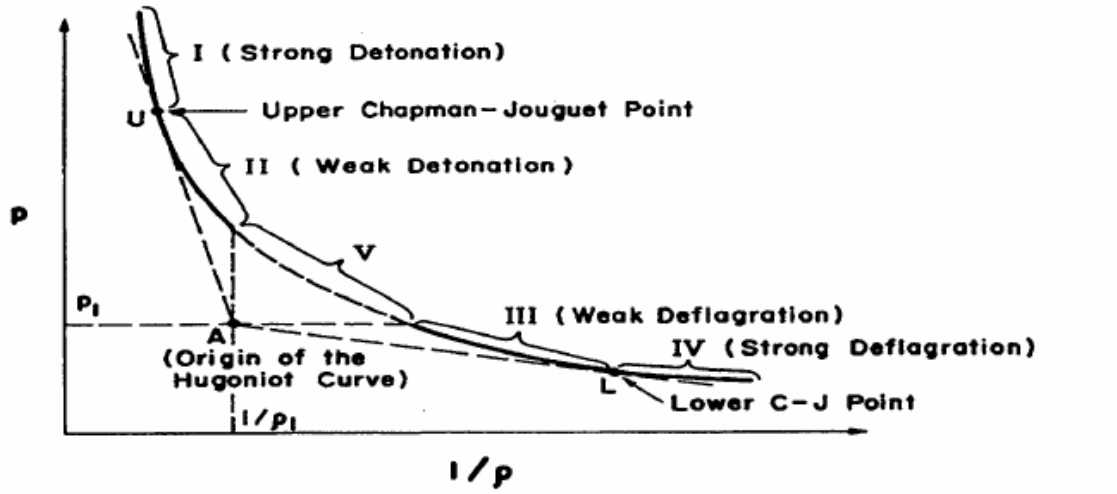

Figure 2. Physical Breakdown of Hugoniot Curve from Ref [2]

Region	Combustion Wave	M_1	M_2
I	Strong Detonation	>1	<1
II	Weak Detonation	>1	>1
III	Weak Deflagration	<1	<1
IV	Strong Deflagration	<1	>1

Table 2. Hugoniot Curve Regional Properties

By differentiating equation (13) with respect to ρ_2, and noting that the Rayliegh and Hugoniot curves intersect at the upper and lower points, the following equation is produced:

$$\frac{p_2 - p_1}{\left(\frac{1}{\rho_1} - \frac{1}{\rho_1}\right)} = \gamma p_2 \rho_2 \tag{24}$$

Combine equations (12) and (13) and setting the result equal to equation (18):

$$u_2^2 = \frac{\gamma p_2}{\rho_2} = c_2^2 \Rightarrow |u_2| = c_2 \tag{25}$$

Which translates to, at the upper and lower C-J points (pts U and L in Figure 2.), the velocity of the combustion products after the wave is limited by the local speed of

sound of the products at the C-J detonation condition even though the detonation wave is moving supersonically relative to the unburned mixture.[5,6]

C. DETONATION WAVE STRUCTURE

A theory for a simplified detonation wave structure was independently arrived at by Zeldovich, von Neumann, and Doring (ZND). They assumed that a steady, one-dimensional flow existed relative to the detonation front and that very limited reactions and heat release occurred in the shock wave itself due to its thickness relative to the mean free molecular path. They theorized that the detonation wave consisted of a planar shock moving at the detonation velocity with chemical reactions occurring behind the shock over a region thicker than the shock wave, and that the shock wave initially heats the reactants to a temperature that can result in a sufficiently fast reaction rate to generate the required energy to support the preceding shock wave. The ZND wave structure can be seen in Figure 3. There are different zones throughout the assumed detonation wave structure. The induction zone immediately behind the shock, where the temperature is not very high, demonstrates a slow increase in reaction rate and relatively flat pressure, temperature, and density profiles. After the induction period the properties change rapidly as the reaction rate increases drastically. The reaction is complete within a distance on the order of 1 centimeter and the properties reach their equilibrium values.

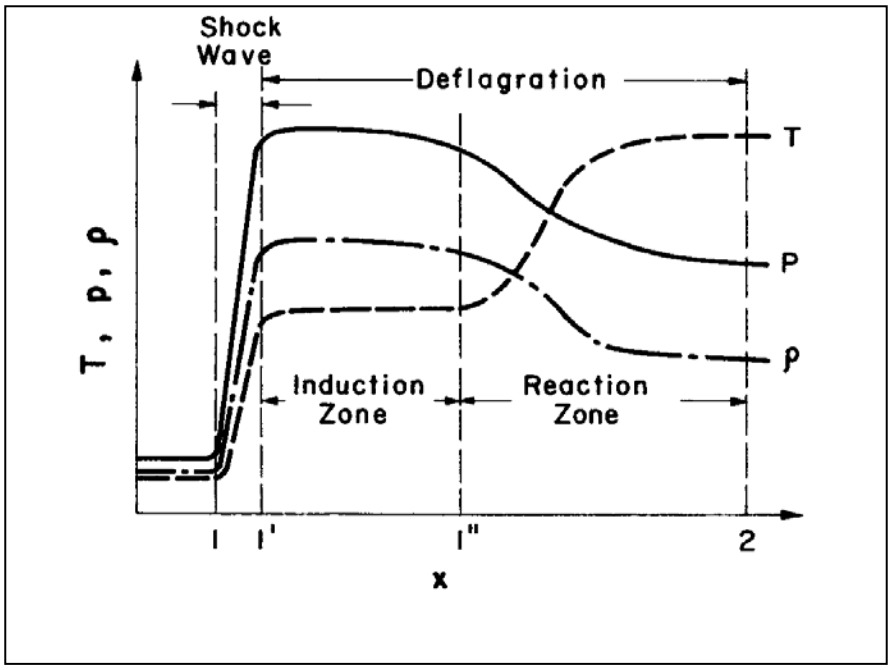

Figure 3. ZND One Dimensional Wave Structure from Ref [4]

Although the ZND model describes a simple detonation wave structure, an actual detonation wave is a three-dimensional structure possessing a complex shock wave structure followed by a reaction zone. The leading shock consists of nearly planar, but curved normal shock segments. At the intersection between these shock segments, lateral shock waves intersect the leading normal shock waves forming 'triple' points. The size of the "fish scale" pattern generated by the triple points of the resulting shock wave structure corresponds to the reactivity of the mixture and is often described by a characteristic length scale, λ. An example of the three dimensional detonation event can be seen in Figure 4. The cell size, λ, is a parameter of practical importance, the more reactive the mixture, the smaller the cell size. The cell size is measured experimentally and there are some variations in the reported results due to the subjective interpretation of the patterns. The transition from a deflagration wave to a detonation wave, the propagation and transmission of a detonation can to some extent be evaluated based on knowledge of the cell size of the mixture.

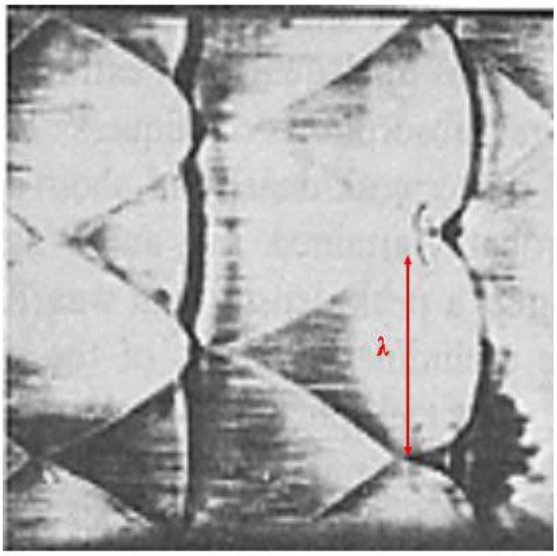

Figure 4. Three Dimensional Cellular Structure

D. THERMODYNAMICS AND PROPAGATION OF DETONATION WAVES

Theoretical cycle analyses have been performed previously to demonstrate the potential performance gain for a C-J detonation process over a constant pressure combustion process using ethylene and air as the reactants. [6]

Determination of the resulting heat addition for both cases was done using the post combustion product conditions generated by the Thermodynamic Equilibrium Program (TEP) for the same given set of initial pre-combustion conditions simulating p=1 atmosphere, T=300 K, fuel/air equivalence ratio of one, flight Mach number of 2.5 at 12,192 m for each case. The synthesis of this work was used in equation (26) to find the heat added, where u_2 is the detonation velocity and c_2 is the sonic velocity behind the wave.

$$\frac{1}{2}\left(u_2 - c_2\right)^2 + C_{P_2}T_2 - C_{P_1}T_1 - \frac{1}{2}u_2^2 = q_{add} \tag{26}$$

To determine the net work and the thermal efficiency, several assumptions need to be made:

(1) The working fluid is both a thermally and calorically perfect gas during isentropic compression and expansion.

(2) The working fluid has constant but different specific heats prior to and after the combustion.

(3) The energy of combustion is determined using thermodynamic considerations contained in TEP.

Equations (2) and (5) and the Perfect Gas Law are used to determine the entropy relationship across the wave was determined using the following relationship:

Entropy $$s = C_P \ln\left(\frac{T}{T_{REF}}\right) - R\ln\left(\frac{p}{p_{REF}}\right) \tag{27}$$

Figure 5. and Figure 6. depict the p-ν diagrams for the Brayton (constant pressure) and detonation combustion cycles. By integrating the area under the under the curve, the net work for each case can be determined. Process 0 to 1 represents a 10:1 compression ratio due to the supersonic flight Mach number and the MIL-E-5007D inlet recovery factor. Process 1 to 2 represents the combustion process, and process 2 to 3 represents the isentropic expansion of the combustion products to ambient pressure. The final step from 3 to 0 is where the remaining heat is rejected to the atmosphere at constant pressure.

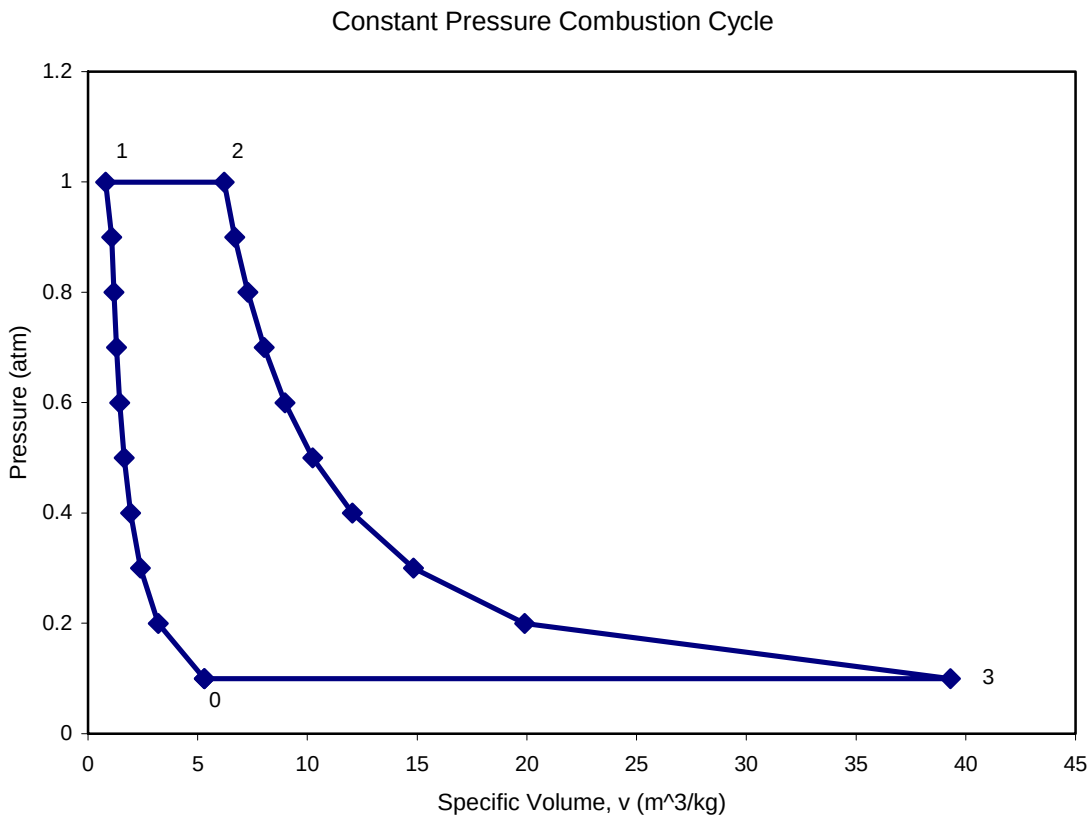

Figure 5. Pressure-Specific Volume Diagram of Constant Pressure Combustion Cycle [Ref 7]

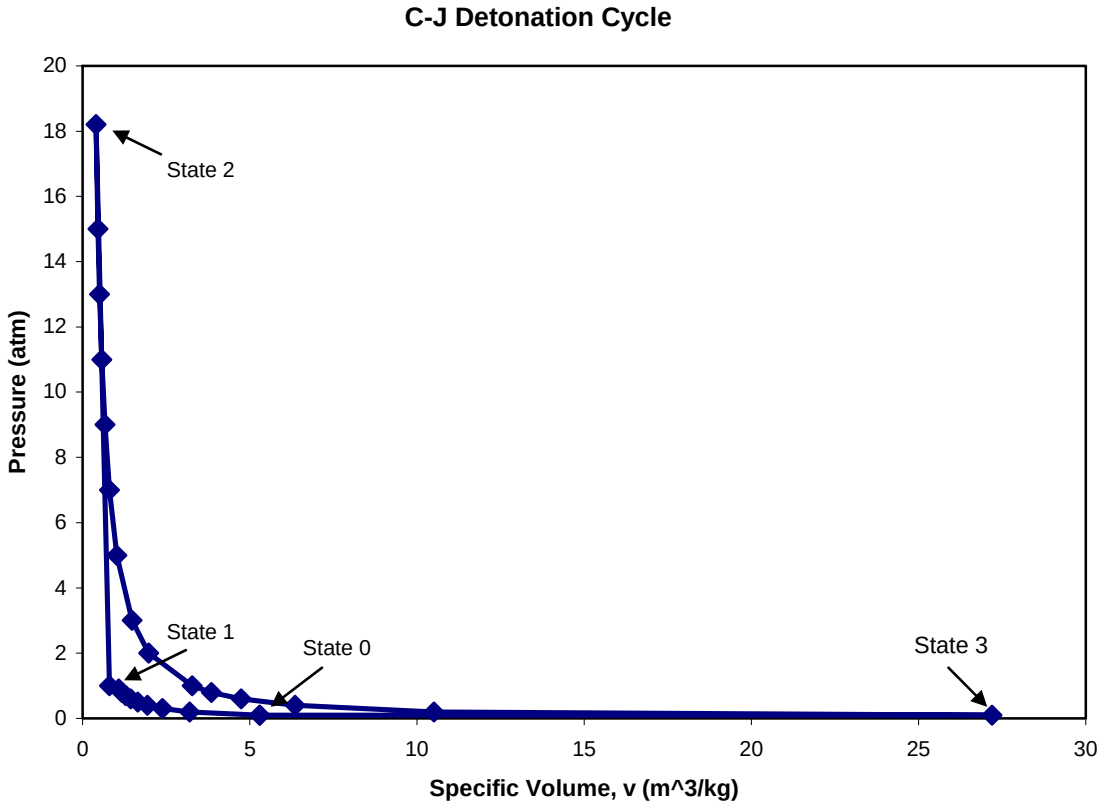

Figure 6. Pressure-Specific Volume Diagram of C-J Detonation Cycle [Ref 7]

The following tables show the conditions used at the various states within the process.

State	Pressure (atm)	Temp. (K)	Specific Volume (m^3/kg)	Entropy (KJ/kg-K)
0	0.1	164.9	5.3	0
1	1	300	0.8	6.5
2	1.0	2256.0	6.6	9.6
3	0.1	1361.1	39.3	9.6

Table 3. Thermodynamic States for a Brayton Cycle [Ref 7]

State	Pressure (atm)	Temp. (K)	Specific Volume (m^3/kg)	Entropy (KJ/kgK)
0	0.1	164.87	5.3	6.5
1	1	300	0.8	6.5
2	17.8	2868	0.47	9.2
3	0.1	1022.9	27.2	9.2

Table 4. Thermodynamic States for a Detonation Cycle [Ref 7]

The net work for each of the processes is found by finding the area enclosed by each of the cycles by integration. The integration is set up for the detonation and Brayton cycles in equations (28) and (29) respectfully.

$$w_{C-J} = \int_2^3 pdv - \int_0^1 pdv - p_0(v_3 - v_0) \tag{28}$$

$$w_{brayton} = p_1(v_2 - v_1) + \int_2^3 pdv - \int_0^1 pdv - p_0(v_3 - v_0) \tag{29}$$

The resulting net work is:

$$w_{C-J} = \left(\frac{p_1v_1 - p_0v_0}{1-\gamma}\right) + \frac{1}{2}\left(\frac{p_2 - p_1}{v_2 - v_1}\right)(v_2^2 - v_1^2) + \left(p_2 - \left(\frac{p_2 - p_1}{v_2 - v_1}\right)v_2\right)(v_2 - v_1) + \left(\frac{p_3v_3 - p_2v_2}{1-\gamma}\right) + p_3(v_0 - v_3) \tag{30}$$

$$w_{Brayton} = \left(\frac{p_1v_1 - p_0v_0}{1-\gamma}\right) + p_2(v_2 - v_1) + \left(\frac{p_3v_3 - p_2v_2}{1-\gamma}\right) + P_3(v_0 - v_3) \tag{31}$$

The thermal efficiency was found by dividing the net work by the heat added for each cycle.

$$\eta_{TH} = \frac{W_{net}}{q_{add}} \tag{32}$$

A graphical representation of the combination of the Brayton cycle and the C-J Detonation Cycle can be seen in Figure 7. and are numerically shown in Table 5.

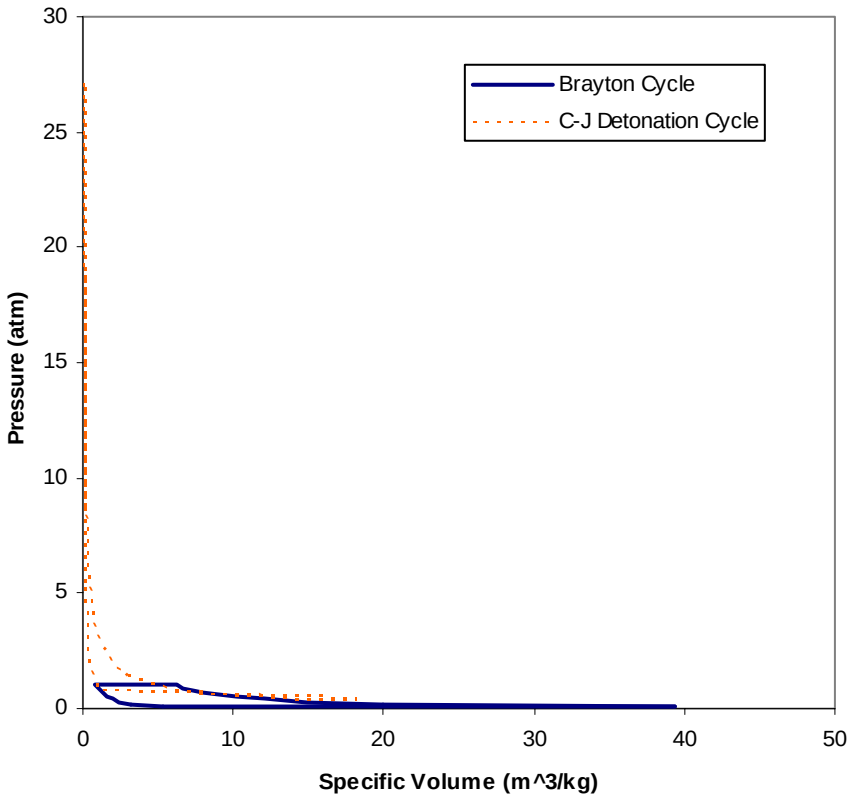

Figure 7. Pressure-Specific Volume Diagram Comparison of C-J Detonation vs Brayton Cycle [Ref 7]

Combustion Cycle	η_{TH} **(%)**
Brayton Cycle	33.8
C-J Detonation	63.7

Table 5. Thermal Efficiencies of the Detonation and Brayton Cycles [Ref 7]

E. EQUIVALENCE RATIO DEFINITION

Equivalence ratio is a term widely used to describe the composition of a mixture used in combustion events. The equivalence ratio, ϕ, is defined as the ratio of fuel-to-oxidizer reactants, divided by the ratio of fuel-to-oxidizer reactants in a stoichiometric ratio; as shown below.

$$f = \frac{\dot{m}_{fuel}}{\dot{m}_{oxidizer}} \tag{33}$$

$$\phi = \frac{f}{f|_{stoichiometric}} \tag{34}$$

A stoichiometric mixture is one in which all reactants are used in the chemical reaction and form complete combustion products. In this study, ethylene, C_2H_4, was used as the fuel and air as the oxidizer. The stoichiometic mixture ratio is represented by the following reaction:

$$C_2H_4 + 3(O_2 + 3.76N_2) \rightarrow 2CO_2 + 2H_2O + 11.28N_2 \tag{35}$$

Since the number of moles of fuel is one and the number of moles of the oxidizer is 3, then the stoichiometirc molar ratio is 1/3 for these reactants. By multiplying each reactant by its molecular weight, the stoichiometirc mass ratio is found to be 0.0679.

F. DETONATION INITIATION

There are three primary approaches used to achieve fuel/air detonations. The first is direct initiation in which a critical mass of the explosive charge is used to initiate a detonation. Direct initiation is not a common process for propulsion applications and there will be no further discussion of this topic in this thesis. A second approach utilizes a strong shock wave to initiate detonations where the existence of turbulence and a shock front are assumed which create the hot spots by the way of shock reflection/focusing,

needed to initiate the detonation. Finally, the third approach utilizes a deflagration-to-detonation transition (DDT) process which accelerates a subsonic combustion wave to the C-J condition. The combustion can be initiated with a low energy spark. The resulting ignition kernel will rapidly accelerate to a detonation through the use of wall turbulence such as tabs or wall spirals within the combustor. DDT has its disadvantages though, which is to include a loss of performance due to the necessity to cool wall turbulence devices, pressure losses during the fill and blow down processes, and difficulty with adequate purging between pulses.

The NPS PDE architecture uses another common approach for detonation. This involves the utilization of an "initiator" which posses a highly detonable fuel/oxygen mixture to generate a strong denotation to propagate a shock wave from one mixture to another less sensitive mixture. This creates an overdriven condition and generally results in a detonation in the main combustor. The main combustor contains a less detonable mixture such as ethylene/air or JP-10/air. The key to this system is the effective transmission of the initiator detonation wave into the fuel/air mixture. This wave must exit the smaller combustor and overcome the diffraction process from initial combustor to a larger combustor diameter and continue to propagate into the main combustor. There is the possibility of re-initiation, due to the reflection of the exiting shock wave downstream of the initiator. The combination of the overdriven initiator and Mach shock reflection has become a proven source of ignition for the NPS pulse detonation engine and was utilized for this test series. [3]

THIS PAGE WAS INTENTIONALLY LEFT BLANK

III. PDE THERMODYNAMICS

A. CYCLE ANALYSIS

One of the primary benefits of a pulse detonation combustion cycle is the calculated higher thermodynamic efficiency and lower entropy rise relative to other combustion processes. The challenges are to establish the flow path timing to ensure that detonation is occurring at the most opportune time and to establish the ideal fuel/air mixture ratio that will maximize I_{sp} for the configuration.

The operational cycle of the valveless PDE is shown in Figure 8. The cycle begins with air flowing through the engine and purging the previous combustion products (A). During the second stage, fuel is injected into the air flow and carried towards the main combustor (B). Stage (C) represents the end of the fuel injection event, and shows the start of the fuel/oxygen mixture into the initiator. The fuel/oxygen mixture is loaded into the initiator and allowed to mixture prior to the ignition (D). Stage (E) shows that the fuel/oxygen mixture has been ignited and a detonation wave is formed. The detonation wave then progresses through the mixture and diffracts successfully into the mixture in the main combustor (F). Stage (G) shows the detonation wave exiting the main combustor with the combustion products remaining behind. Finally, after the detonation wave exits the main combustor, a series of rarefaction waves reduce the pressure inside the combustor and the combustion products are purged from the engine (H).

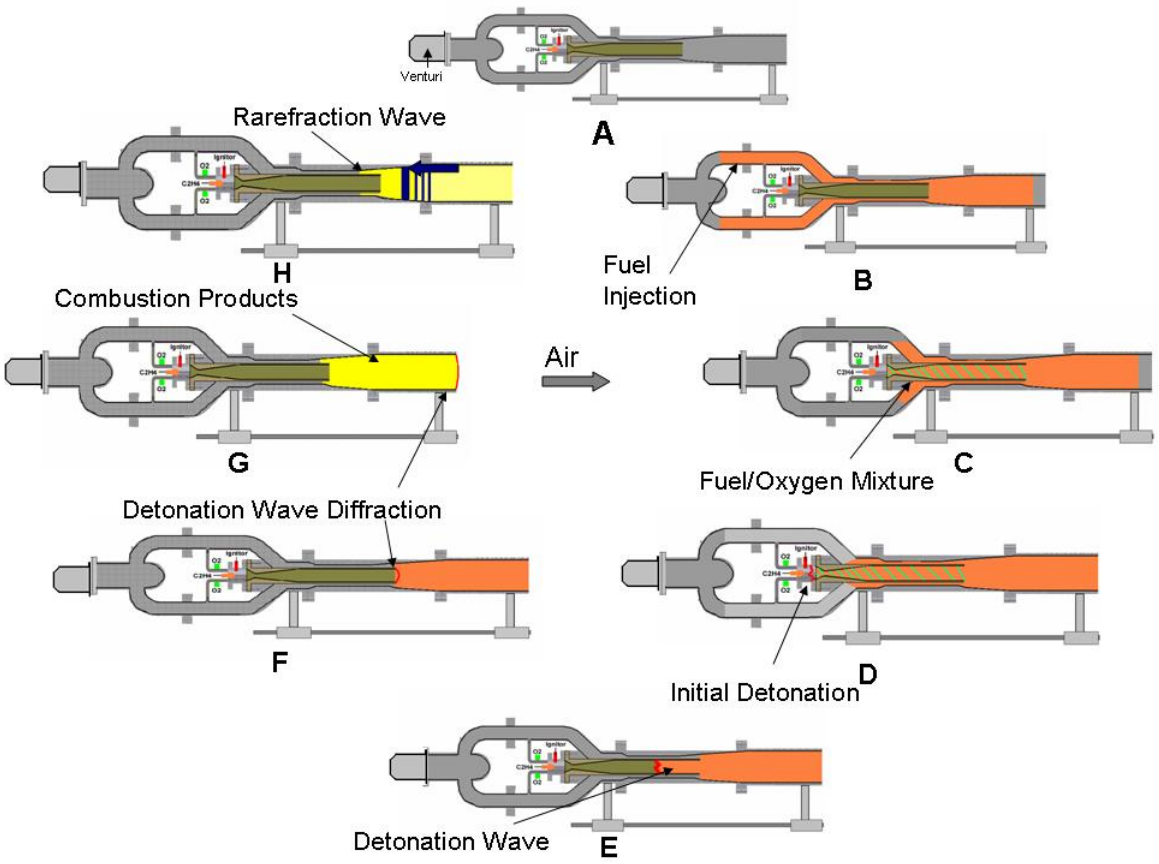

Figure 8. Valveless PDE Cycle

Immediately after the initiator detonation wave diffracts into the main combustor, a combustion-driven shock wave begins propagating upstream into the incoming air stream. This propagation can be minimized/eliminated if the velocity of the incoming air is sufficiently high and results in a choke point somewhere in the isolator, thereby producing a supersonic flow regime immediately downstream of this point. The degree of isolation the isolator provides does affect performance due to a total pressure recovery loss. The optimum amount of isolation is being evaluated computationally within the ONR PDE Research program.

B. MULTI-CYCLE EFFECTS

As discussed in prior sections, a typical single detonation cycle consists of loading a fuel/oxidizer mixture, ignition of that mixture, propagation of a detonation

wave down the tube, and the products being expelled from the tube by rarefraction waves created by the sudden expansion to atmospheric pressure after the detonation wave exits. Ideally, this cycle could be repeated at a very high cycle frequency without having to account for each cycle's effect on the next and without affecting the performance of the engine. In reality, there are several key issues, delineated below, that need to be accounted for in order to ensure engine performance.

First, the thrust developed by the engine can be determined by either measuring the momentum flux out of the engine or by integrating the head-end pressure over time if a convenient thrust wall exists. The average thrust can actually be reduced due to the expansion below atmospheric pressure after the detonation wave exits the combustion tube. Proper coupling of the next cycle's fuel/oxidizer loading sequence to the end of the previous cycle can be used to eliminate the effect by preventing the pressure within the tube form dropping below the local atmospheric value. The valveless detonation engine geometry which utilizes a continuous mass flow rate of air, similar to a jet engine, nearly eliminates the effect.

Second, the cycle repetition rate, or frequency, is limited by the physical size of the detonation tube, the finite times required for loading the reactants, timescales for the DDT process, and purging the products. The aggregate air mass flow rate, which is a function of the flight conditions, strongly dictates the operational cycle. A valveless engine design shortens the product purge time, thereby theoretically increasing the potential cycle frequency.

Third, the importance of matching the fuel/oxidizer load time of the next cycle to the detonation wave exit of the previous cycle must be balanced against the possibility of the new mixture to prematurely ignite due to remaining products of the previous combustion event still present in the tube. This possibility will again limit the cycle frequency and could affect the maximum average thrust produced by the engine.

THIS PAGE WAS INTENTIONALLY LEFT BLANK

IV. EXPERIMENTAL SETUP

A. VITIATOR

A hydrogen/oxygen vitiator was used to increase the "inlet air" temperature of the engine to temperatures approaching 533 K (500 ˚F). This was done to simulate the typical inlet conditions that a pulse detonation engine would experience in-flight at nominal supersonic flight conditions expected for such a system. Compressed air was routed into the vitiator, were an H_2/O_2 igniter was used to light a self-sustaining hydrogen/air combustor. Since the vitiator combusts externally provided hydrogen and oxygen in the air, 'make-up' oxygen is added downstream of the vitiator to ensure that the 'inlet air' is brought back the proper oxygen molar concentration of 21%. A picture of the vitiator can be seen in Figure 9. The vitiator can maintain engine inlet temperatures ranging from 50°F to ≈ 450 °F depending on the desired test conditions.

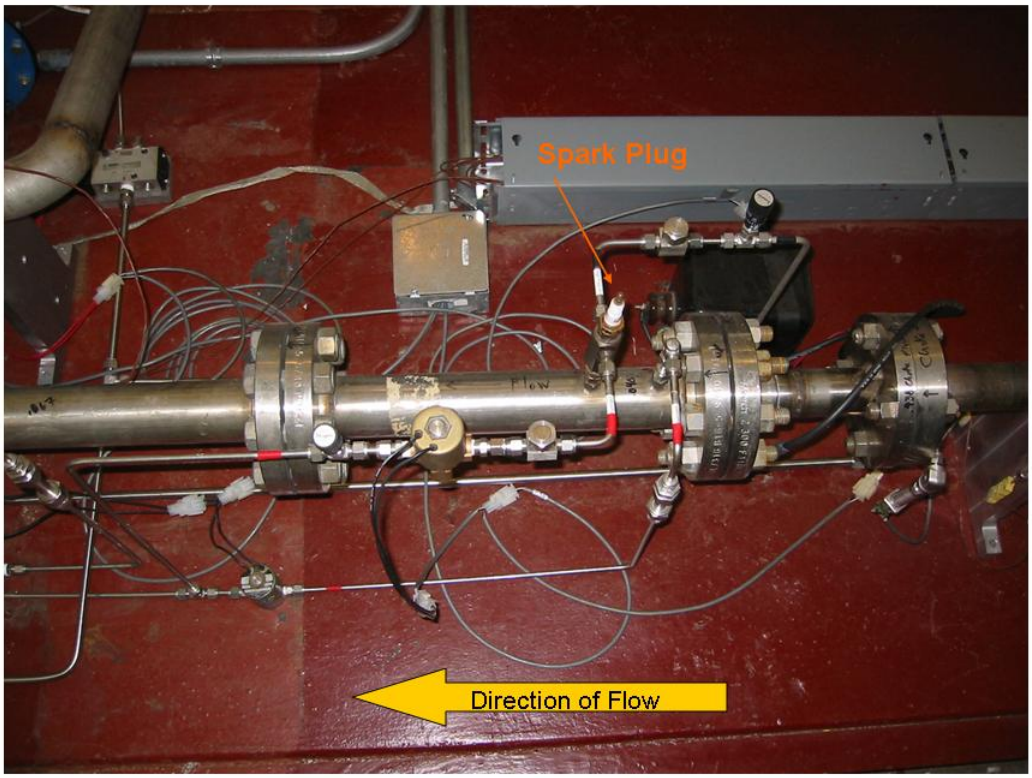

Figure 9. Hydrogen/Oxygen Vitiator

B. PULSE DETONATION ENGINE

The major portion of this thesis was the modification of the Naval Postgraduate School's pulse detonation engine installation to incorporate a six degree-of-freedom test stand designed by Pacific Press and new control and data acquisition system. The cell was stripped of all previous plumbing and electrical wiring. The new thrust stand was positioned and a back brace was designed and connected to the stand to allow for a perpendicular brace for alternate thrust measurements through a spring/displacement system and as a support bulkhead for the tubing connections. The drawings for this piece can be found in Appendix E. The test set up can be viewed in Figure 10. The geometry under development at NPS is a continuous air flow design, which does not utilize or require valves to supply air to the main combustor chamber as shown in Figure 11. Air flow is monitored and restricted by a converging/diverging inlet venturi, with a 16.6 mm throat diameter, at the forward end of the PDE.

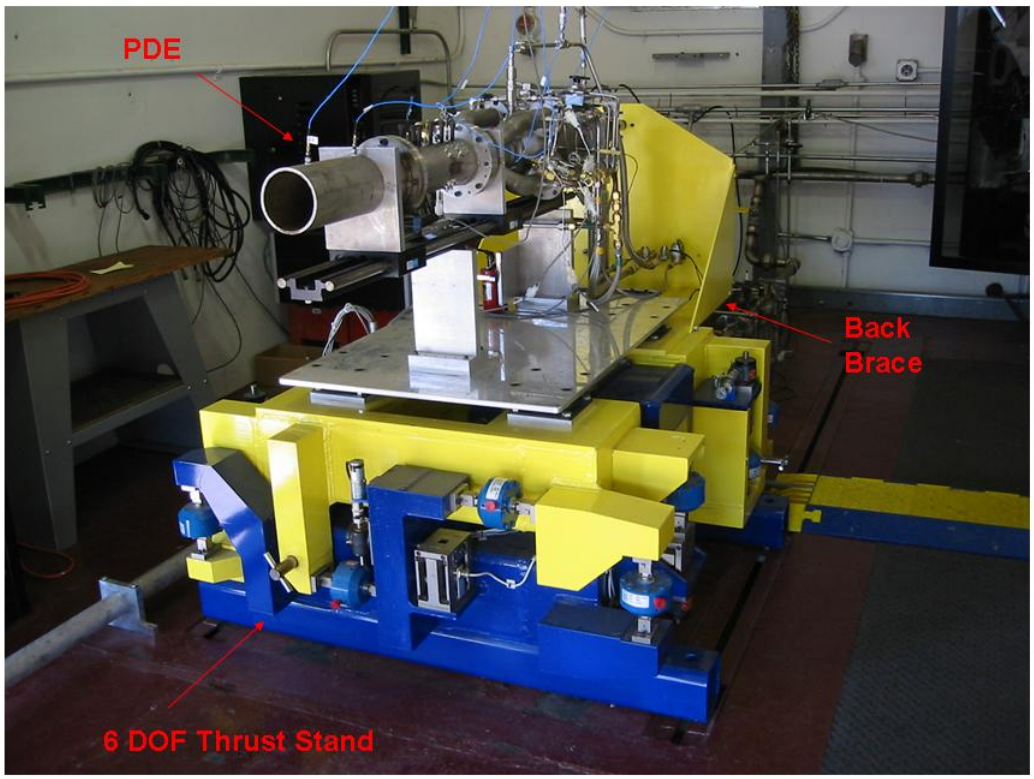

Figure 10. NPS PDE Test Cell #2

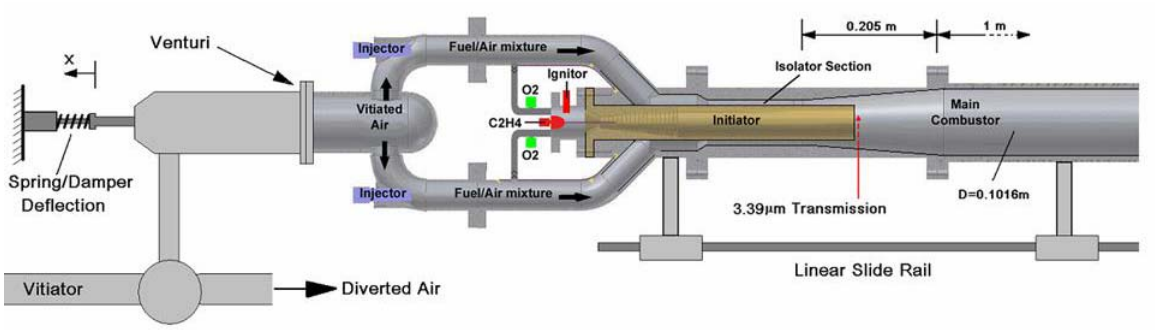

Figure 11. Schematic of the Valveless NPS PDE [Ref 3]

The design consists of four fuel/air inlet arms which discharge into a common inlet manifold. The requirement for these arms for operation is only that they provide adequate length for good mixing and for liquid fuel to vaporize prior to the main combustor entrance. The optimal inlet arm length will be determined through additional computational studies. Additional drawings of the NPS PDE can be seen in Appendix A. A detailed view of the test set up can be viewed in Figure 12. The fuel injection delivered by Valvetech solenoid valves (15060-2) which are controlled by a BNC 5000 pulse generator.

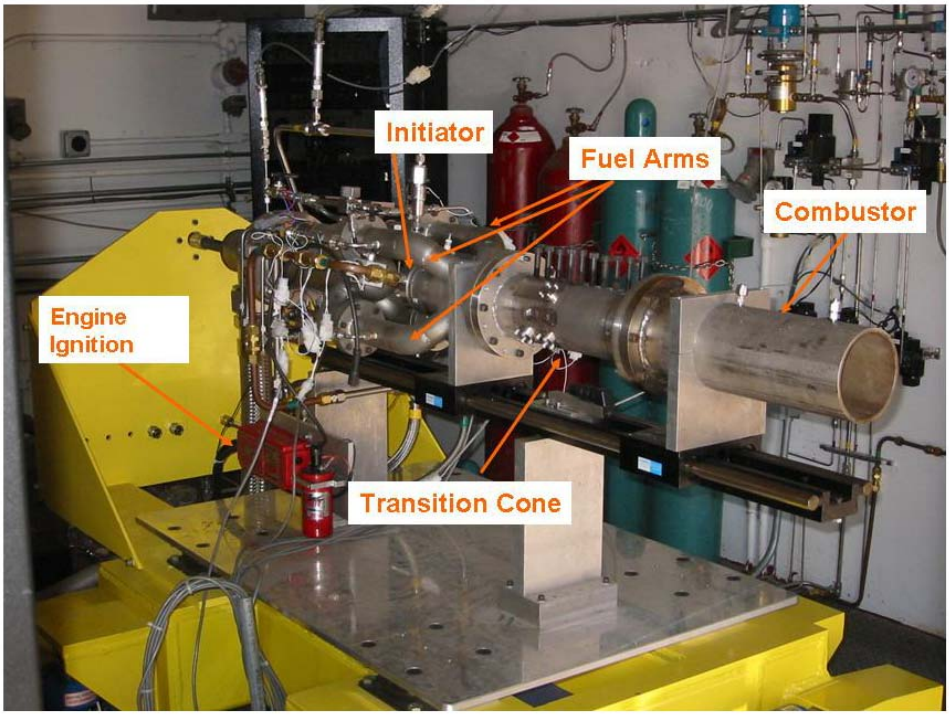

Figure 12. NPS Pulse Detonation Engine

C. INITIATOR

The initiator is a .254 m long stainless steel chamber with a varying head-end cross-section, with an internal diameter of .04445 m. The geometry for this initiator was previously developed from research performed by LT Dave Forster on initiating detonations and can be seen in Figure 13. [5]

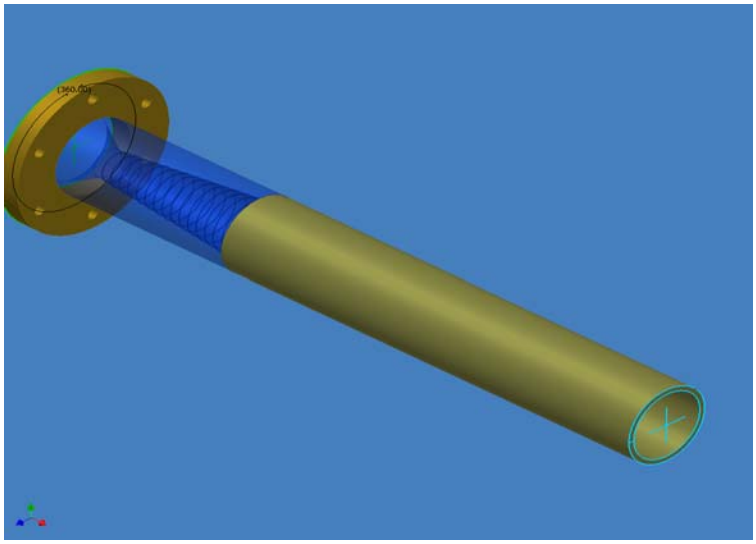

Figure 13. Solid Model of Initiator

Purge air continuously flowed through the initiator during operation and provided approximately 20% of the oxidizer required for operation of the initiator. Oxygen and ethylene were then injected at appropriate intervals before the initiation of a detonation in the initiator. Oxygen was injected into the initiator with Parker Hannifin Valves (009-0449-900) and ethylene was injected using a Valvetech (15060-2) valve.

D. EXHAUST TUBE/ SILENCER

An exhaust tube was used to direct the exhaust gases from directly behind the engine to a location 0.508m beyond the test cell. The tube also doubled as a noise suppression system to help reduce the level of noise introduced into the local environment. A noise suppression system was also installed using water misters as shown in Figure 14. to further aid in the suppression of the resulting engine noise.

Figure 14. Noise Suppression System

Location	Exhaust Tube Only (dB)	Full Noise Suppression System (dB)
1	127.133	125
2	129.1	125
3	121.56	113.5

Table 6. Noise Suppression Results

Table 6 shows the noise level readings taken with and without the noise suppression system engaged.

Location 1 is located behind the exhaust tube at the edge of the property line (approximately 91 m). Location 2 is that same location, but at an approximate height of 7m. Location 3 is approximately 70 m from the forward end of the engine. As shown in Table 6, the noise suppression system slightly decreases the noise produced by the system.

E. FACILITY CONTROL

A major effort of the Naval Postgraduate School PDE program this year was the development of the new facility control and data acquisition system. The control and data acquisition system was run on a PC using software by National Instruments called LABVIEW 7.1. The control system hardware for the program was run on the PXI 1000B controller using the LABVIEW RT (real time) system. This is a non-Windows based system that had the advantage of lower overhead than an application based on a Windows environment. The control program was semi-automated, requiring the user to open supply ball valves and set the engine and vitiator parameters prior to starting the vitiator and running the engine. The vitiator sequence was automated for both safety and time restrictions. Finally, the engine control was performed by a BNC pulse generator which allowed for separate control of the engine cycle that allowed for the real time modification of the engine operating frequency. The facility control GUI (graphical user interface) is shown in Figure 15. The facility was controlled using the Digital Output lines from the PXI-6031E to enable CRYDOM solid state relays. A PXI-6508, a 96

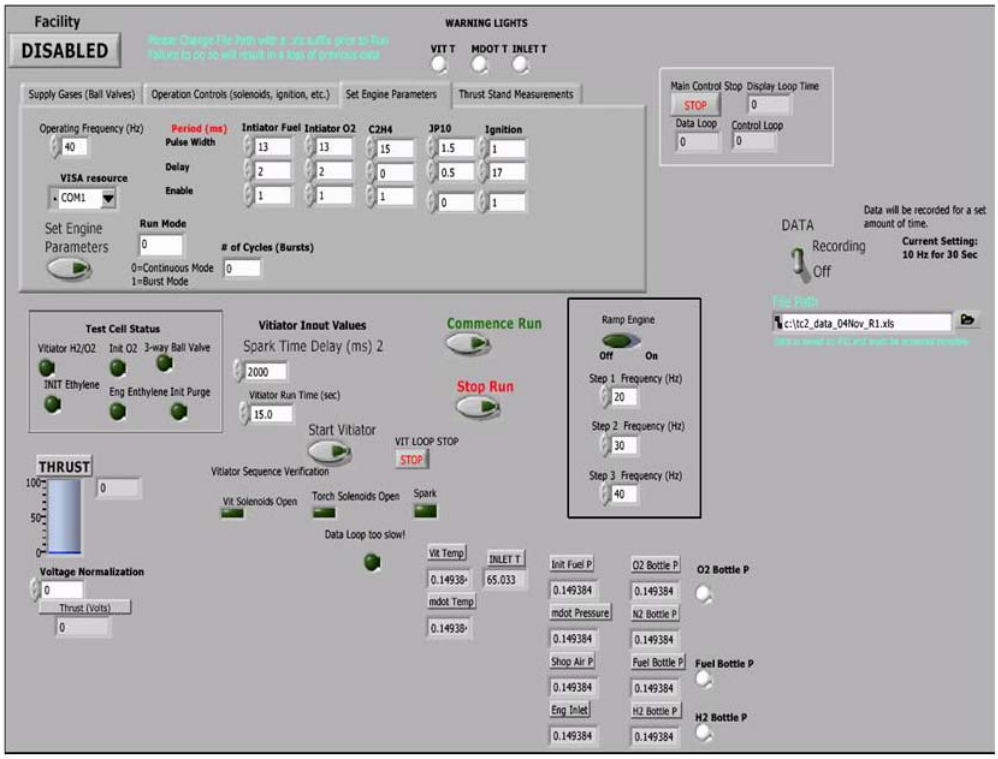

Figure 15. Test Cell #2 GUI

channel digital input/output board was also used for specific relay control. Photographs of this system can be seen in Appendix D.

The GUI was also designed to take low speed (10 Hz) facility data that is used to monitor various pressure transducers placed on both supply gases and at various location on the engine as well as various temperature on the well as being recorded for future viewing. The PXI 6031E, 16-bit Analog Input card in engine and air lines. This information is displayed on screen in a real-time capacity as differential mode was used to collect this data. An example of the data recorded for the facility can be found in Figure 16.

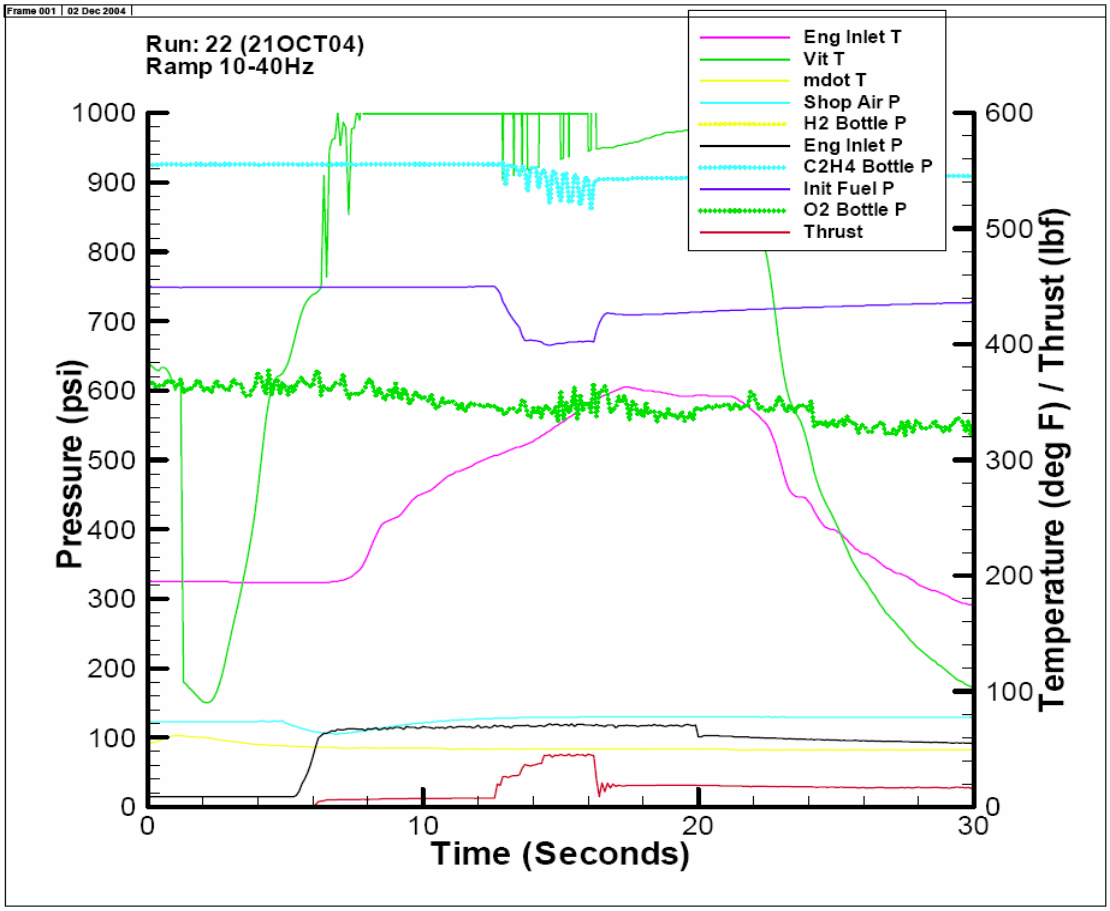

Figure 16. Example of Facility Pressure and Temperature Data

F. HIGH SPEED DATA AQUISTION

Kistler 603B1 pressure transducers were placed along the PDE, which were used to monitor detonation/shock wave speeds. The locations of these transducers both along the main combustor and upstream of the fuel injection location can be seen in Figure 17. To collect this data at 500 KHz per channel a second PXI-1000B which housed three PXI 6115 high speed DAQ cards, was dedicated to measuring the pressure transducer data. The data acquisition system recorded up to 6 channels of data which is both viewed on screen after the test and written to a file for further post processing. The GUI used for the high speed data acquisition was an existing data logger from NI seen in Figure 18.

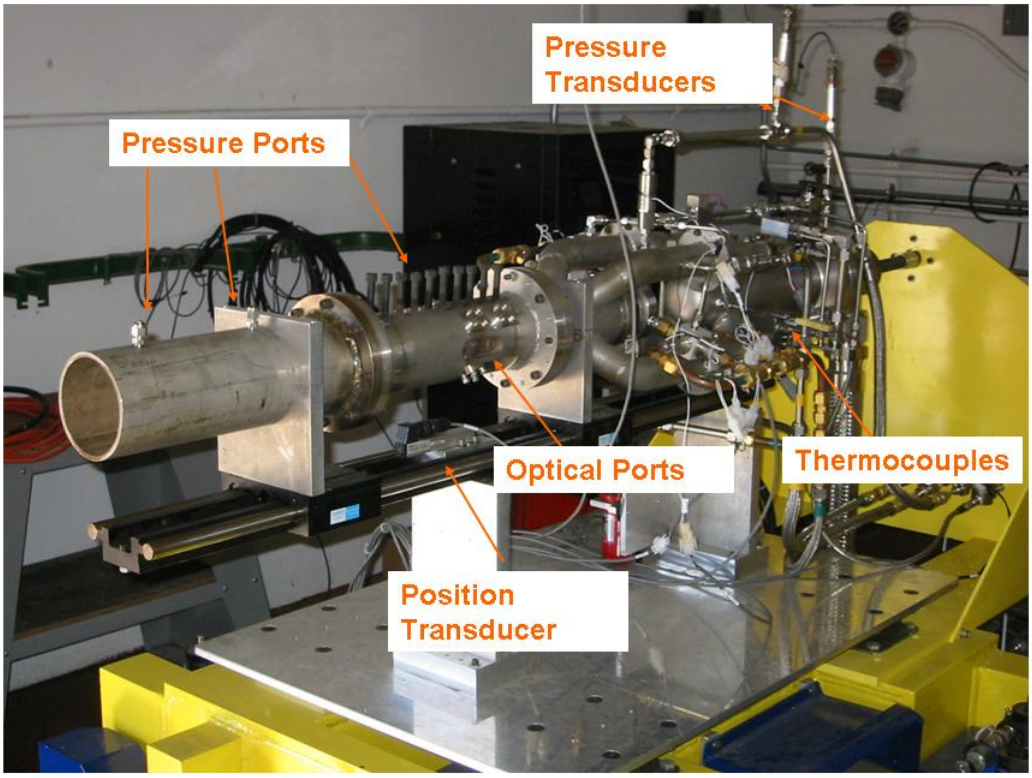

Figure 17. Transducer Locations

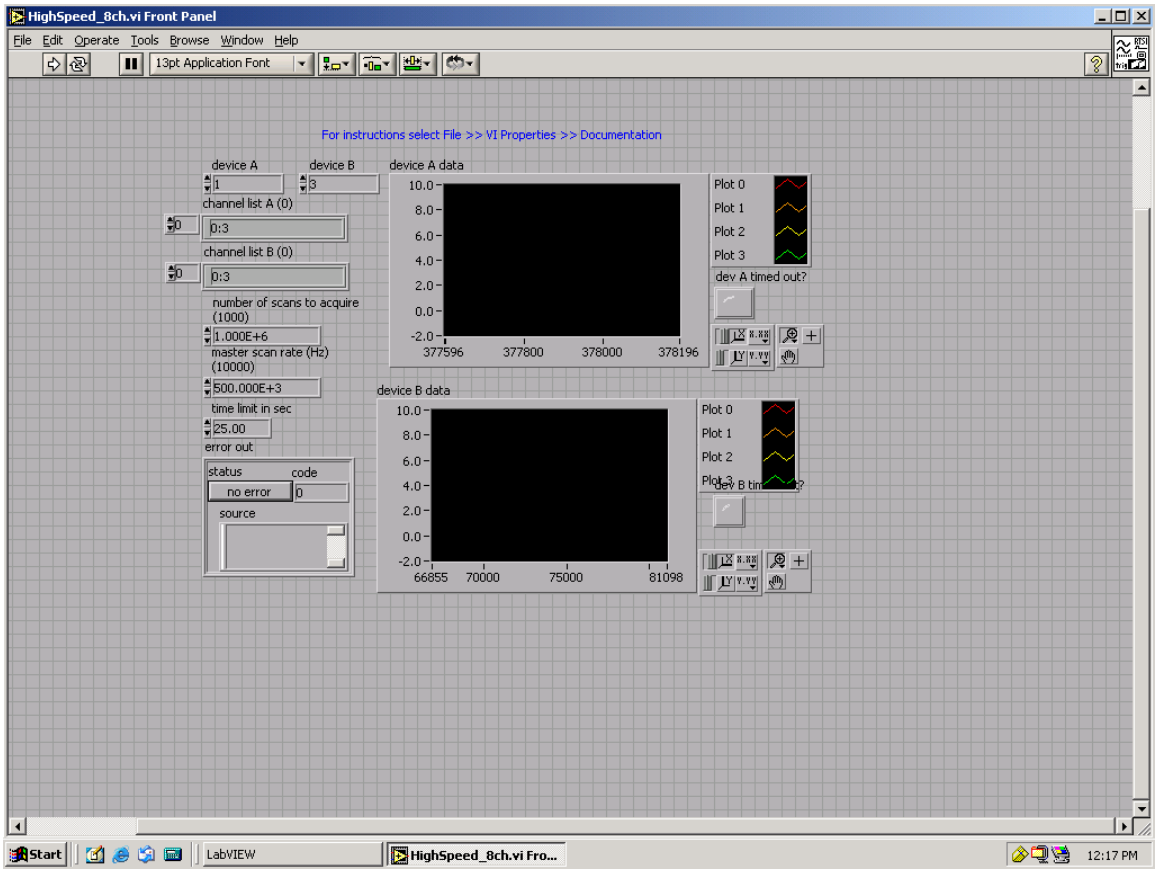

Figure 18. High Speed DAQ GUI

Due to the limitations of both the hardware and software, typically only one second of data at this acquisition rate could be recorded. An example of this data is shown below Figure 19.

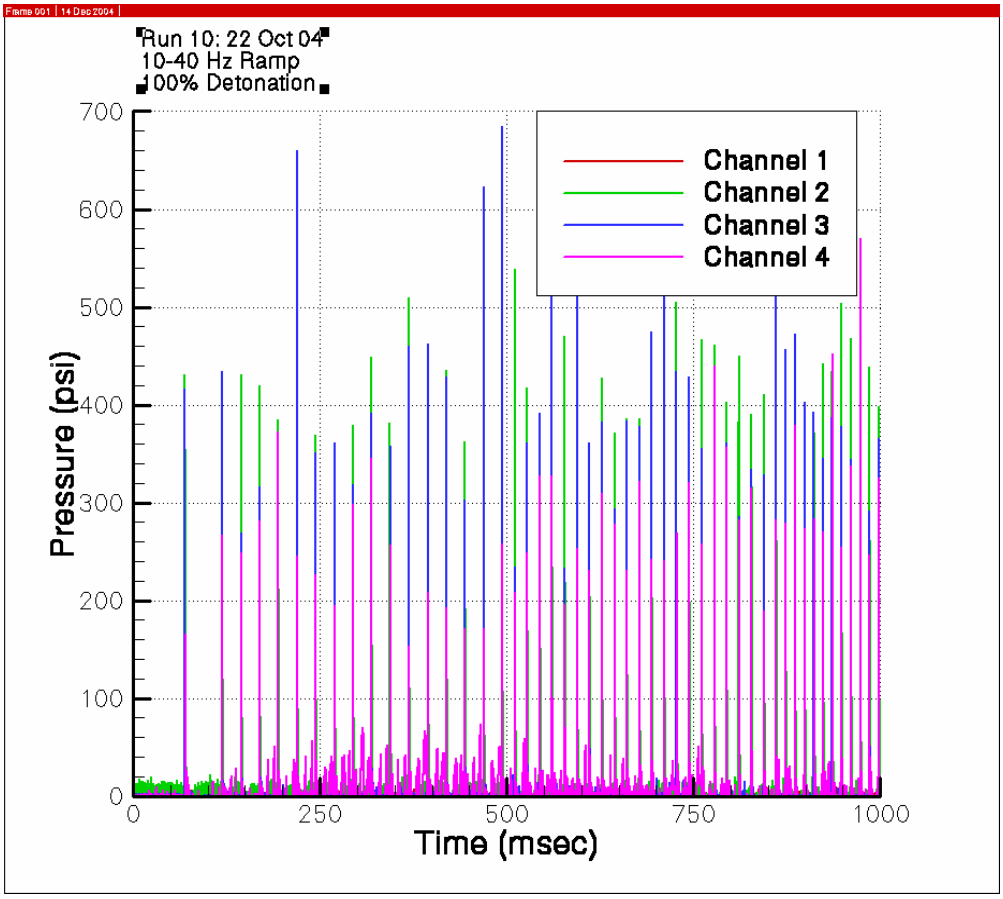

Figure 19. Example of High Speed Pressure Data

G. THRUST MEASURMENT

A thrust measurement independent of the thrust stand was used to calculate the force from the NPS PDE. This was accomplished using a NOVOTECHNIK position transducer w/restoring spring (TRS 75) as can be seen in Figure 17. The control program GUI can record either direct voltage output or will convert this voltage into a force measurement using the calibration curve presented in Appendix C. The curve was created after pressurizing the air delivery system, to account for tare loads due to pressurization of the flex lines. This process can be viewed in Figure 20.

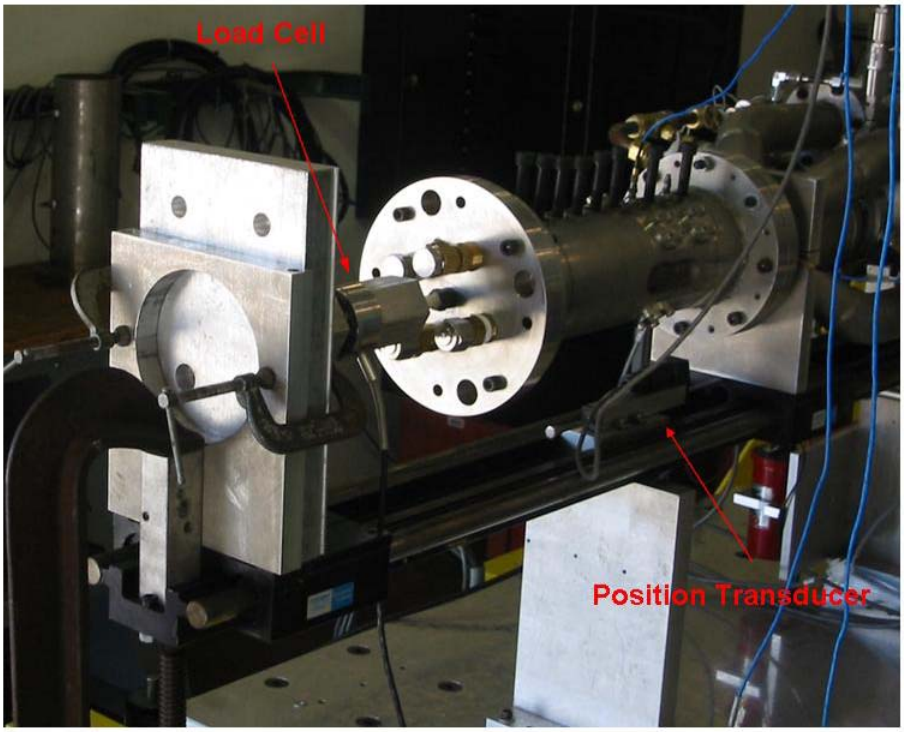

Figure 20. Position Transducer Calibration

H. OPTICAL FUEL MEASUREMENT

The Naval Postgraduate School is currently developing the diagnostic capability on-site to acquire a temporal fuel data, however Stanford University is jointly participating in this research and performs this role as they continue their refinement of the use of tunable diode lasers (TDLs) for water temperature and fuel measurements. This process is shown in Figure 21.

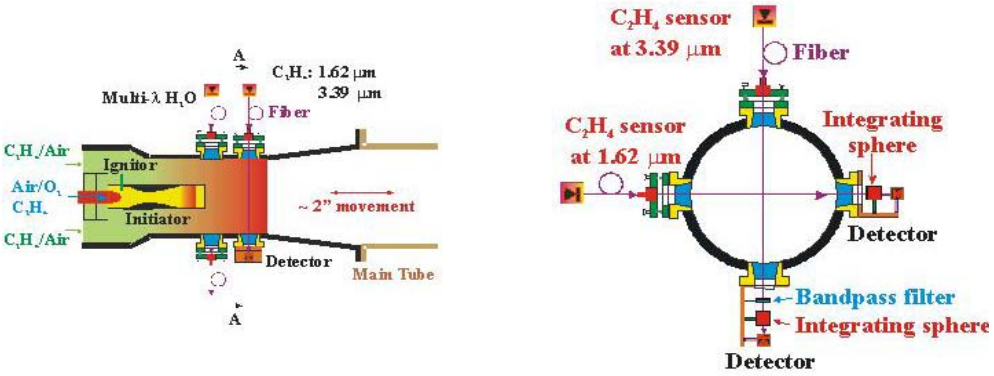

Figure 21. Tunable Diode Laser Test Setup

This technique has been proven to measure temperature and fuel measurements for speeds ranging from 10-50Hz. The laser diagnostics have been engineered to tolerate movement, vibration, beam steering, and emission in the harsh environment present in the PDE. Specifics for this technique can be found in Reference [8]. The actual setup used at NPS can be viewed in Figure 22.

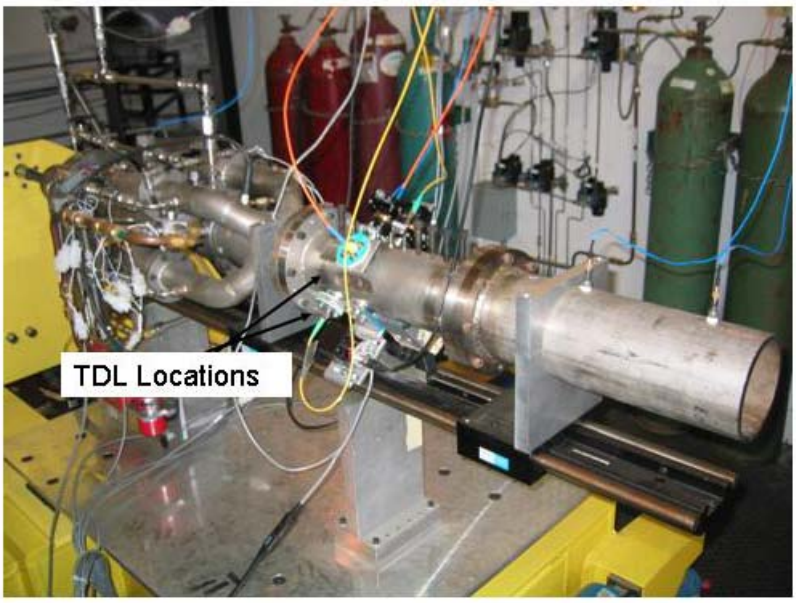

Figure 22. Tunable Diode Laser Setup on PDE

V. RESULTS

A. PERFORMANCE TESTING

Equation (1) describes the effectiveness of an air-breathing engine as a performance relationship between the net force created and the mass of the fuel used to generate that force or thrust. The challenge in evaluating performance during any test program is to develop high fidelity measurement capabilities for both force and mass flow. This becomes especially difficult when dealing with unsteady flow such as those related to PDEs.

1. Fuel Injection Characteristics

A very important measurement in determining the specific impulse of a PDE is the temporal fuel profile of the fuel injection into the engine. The existing fuel distribution along the engine axis at the time of detonation directly affects performance. Prior research was conducted which utilized calibrated choked orifices to determine the fuel mass flow rate needed for I_{sp} calculations. Tunable Diode Lasers (TDLs) are now available that allow for quantitative temporal fuel measurements. This leads to a detailed fuel distribution profile which in turn produces a higher fidelity I_{sp} calculation for the engine. An example of the fuel injection data that the Stanford team was able to collect during testing can be seen in Figure 23.

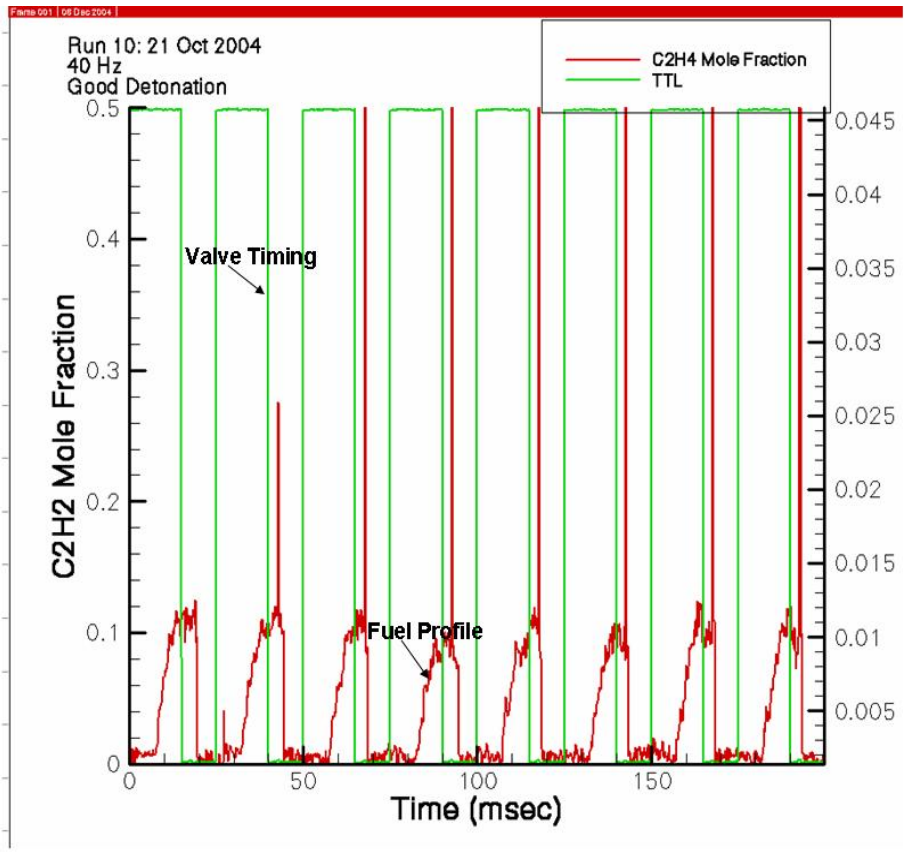

Figure 23. Example of Fuel Profile Data from TDLs

This data is critical for determining an accurate fuel mass flow rate profile during the detonation. In order to do this, the velocity (V(x)) within the combustion tube is calculated solving the following equation for V(x).

$$\dot{m} = \left(\frac{p}{RT}\right)\left(V(x)A(x)\right) \tag{36}$$

Once the velocity distribution of the fuel/air mixture was calculated, the average time to fill the main combustor could then be determined. The fill time was then used to determine the average fuel fill profile distribution along the combustor. The nominal fuel profile was created by averaging the data from the eight shots recorded over the fill time calculated. The measurement portion is shown in Figure 23. and was used for the mass calculation of C_2H_4 in the main combustor. This however is not the total "fuel" to be accounted for in the system when determining the fuel-based I_{sp}. The auxiliary oxygen

added to the system initiator must also be included in the total mass of the fuel used in the denominator of equation (1) since it was considered as a weight and volume penalty on the actual system. The total mass of fuel in the system is therefore calculated by:

$$m_f = m_{C_2H_4} + m_{O_2\_Aux} \tag{37}$$

Clearly, the auxillary oxygen used in the initiator will reduce the system specific impulse calculation and will need to be eliminated on future versions of the engine.

2. Thrust Measurements

The next step in determining the performance of the engine was to calculate the net force (F_{NET}, eqn (38)) that was produced by the system.

$$F_{NET} = F_{Gross} - F_{RamDrag} \tag{38}$$

Prior to calculating the net force, it was important to first confirm that a detonation had occurred. This was confirmed by calculating the wave speed in the main combustor. The transition time between channels 3 and 4 of the Kistler 603B1 pressure transducers was measured (see Figure 24.) and knowing the distance between the two transducers, the wave speed could then be calculated. The wave speed was then compared to theoretical values on Figure 25. to ensure that a detonation had occurred.

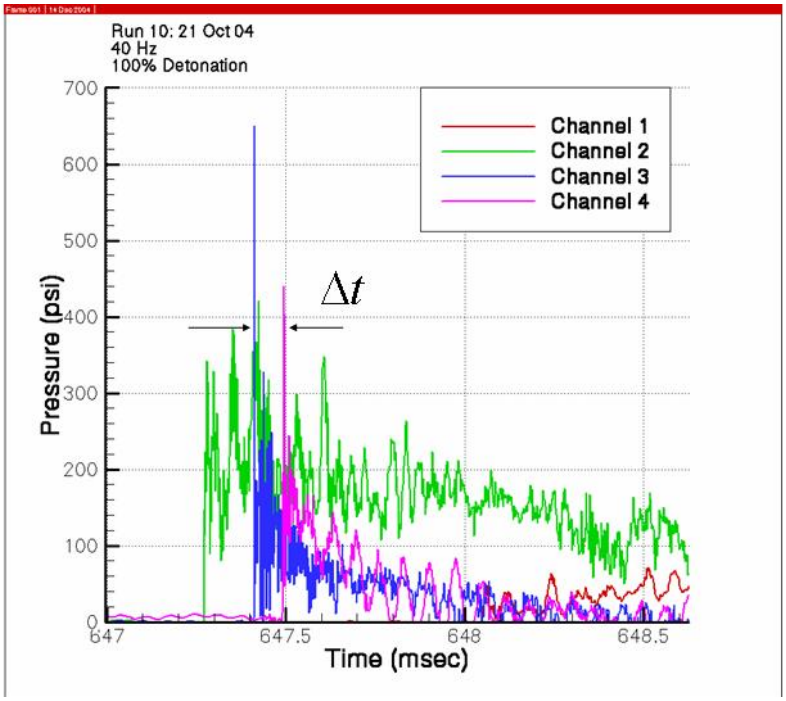

Figure 24. Example of Detonation Wave Transition

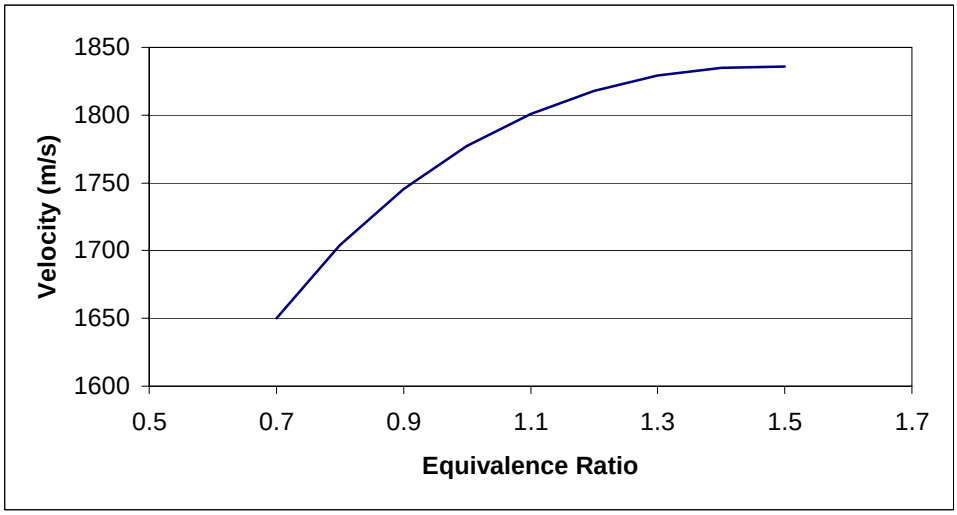

Figure 25. Theoretical Detonation Wave Speeds

The gross force (F_{gross}) was calculated from the displacement measurement recorded from the linear position transducer. Ram drag needed to be subtracted from this force to account for the inlet momentum flux delivered to the engine.

3. Specific Impulse Calculations

The specific impulse of the PDE was then calculated using equation (1) and revealed the I_{spf} of 1106.1 sec at an equivalence ratio of 1.27 at the test settings seen in Table 7. Figure 26. is a compilation of numerous PDE runs from various researchers. As shown in the graphic, the NPS PDE falls amongst the majority of these engines. An important advantage of the NPS PDE is that it is a valveless system, making it simpler and likely more cost effective. Most of the remaining data on the figure is for systems which include valves on the air delivery systems.

Frequency	mdot(air)	mdot(fuel)
40 Hz	0.33 kg/s	0.02244 kg/s

Table 7. Nominal Test Settings

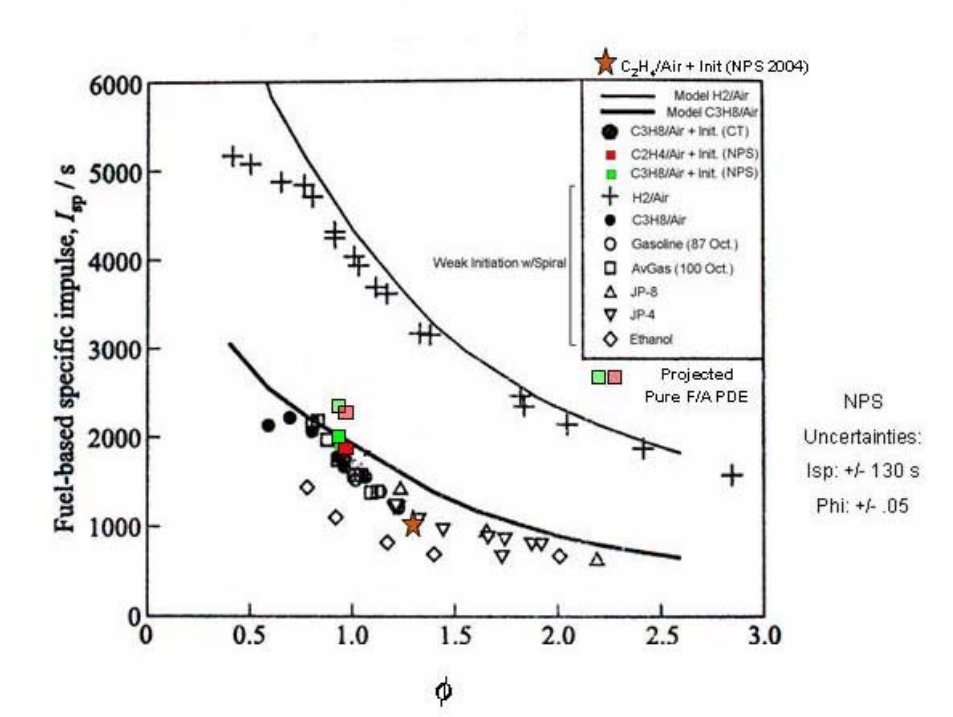

Figure 26. Specific Impulse-Equivalence Ratio for PDE

The multiple NPS data points on the graph represent both the current geometry as well as a longer combustor configuration evaluated preciously. In previous testing of the NPS PDE, the main combustor was over twice the length of the one currently installed on the test stand. This resulted in a smaller initiator/main combustor volume ratio for the

previous runs which would lower the effect of the auxiliary oxygen on the overall system performance. Previous testing calculated a ϕ of 1.0 or less while tests run for this thesis were at a ϕ of 1.27 which meant the engine was not being run at its ideal settings, resulting in the lower specific impulse values. Although only one test condition is presented in Figure 26. it is representative of all the performance runs made at 40 Hz.

VI. CONCLUSIONS

The integration of a six degree of freedom thrust stand with independent linear-displacement force measurement capability and optical diagnostics for fuel mass injection characteristics was performed to allow for two independent measurements of thrust and fuel flow rates for specific impulse performance measurements. The successful application of the optical fuel measurement system using TDLs demonstrated the advantages of quantitative temporal fuel profile information. The results allowed for the fuel distribution to be accurately determined, resulting in an equivalent combustor fuel mass loading for specific impulse calculations.

The successful design of the 'smart' real time control system for the PDE allowed for the automation of the overall system. This produced the ability to actively vary the engine operating parameters during a run in the attempt to find the ideal run parameters for maximizing performance. This system was used to demonstrate operational frequencies of up to 50 Hz on the valveless geometry.

Finally, the integration of the aforementioned systems has allowed for high fidelity performance data on the valveless engine PDE geometry at a fixed condition. The data will be provided to researchers within the ONR PDE Research program to aid in the proper modeling of the NPS system and aid in the continued development/evolution of the NPS PDE architecture.

THIS PAGE INTENTIONALLY LEFT BLANK

APPENDIX A NPS PULSE DETONATION ENGINE DRAWINGS

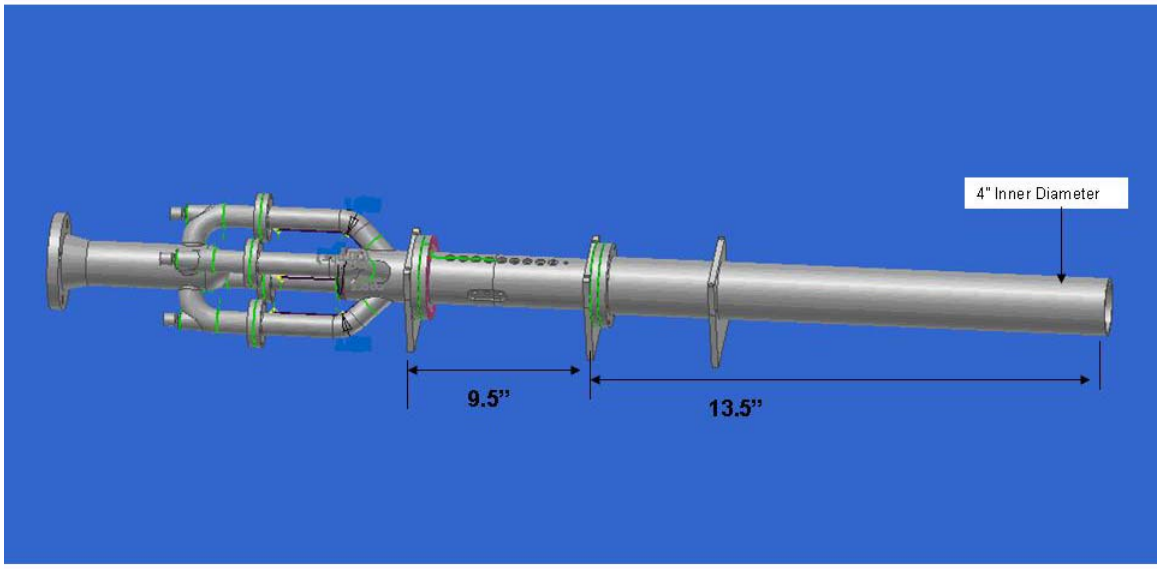

Figure 27. NPS Pulse Detonation Engine

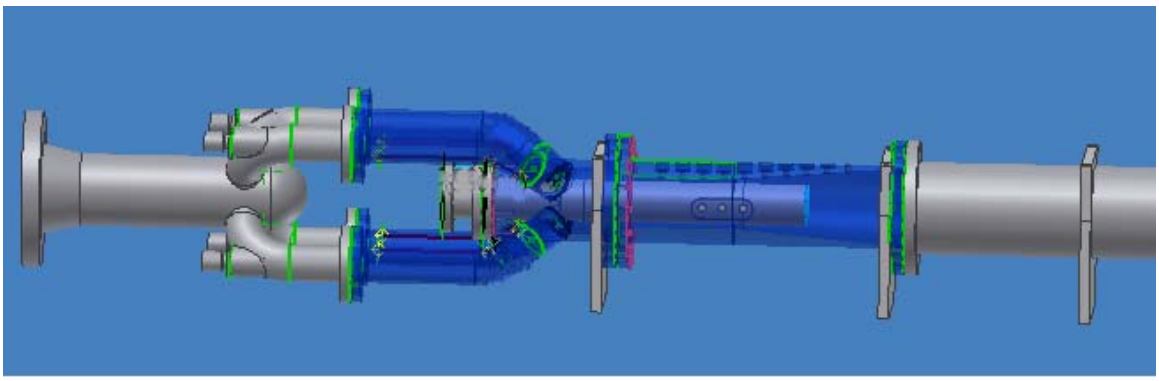

Figure 28. Internal view of PDE Initiator, Diffraction Plane, and Main Combustor

THIS PAGE INTENTIONALLY LEFT BLANK

APPENDIX B TEST CELL STANDARD OPERATING PROCEDURES

Test Cell #2
Standard Operating Procedures (S.O.P)
Engine Start UP
(last modification date 01 December 2004)

Prior to starting preparations

1. Notify all lab personnel of live test cell.
2. Turn ON warning lights
3. Notify the Golf Course (x2167) (Only required if Hot Fire Test is conducted)

Preparing Test Cell

1. Push the Emergency Stop IN (secured)

2. Ensure MSD Ignition OFF (disarmed)
3. Ensure that PXI Controllers, Amps, Kisslers, and Power strips in 2 the black cabinets are ON.
4. On Scarp, open LABVIEW and ensure that the execution target contains the PXI address. Open control panel and run the program.
    a. RT Target address: 169.254.0.2
    b. Control Program Path
        i. Open
        ii. Test Cell #2 Manual Control v16
        iii. Enter Run Path Name
            1. If this is not completed prior to running you will lose the data file that was created with the default name.
5. On Savage, switch view to PXI in windows mode.
    a. You are using LabView not RT
    b. High Speed DAQ Path
        i. Open on Desktop High Speed (8 Channel)
        ii. Ensure that you are set on the external trigger.
        iii. Ensure Device A set to 1, Ensure Device B set to 3
        iv. The vi has the ability to take two seconds of data and will from the moment that it receives the trigger. The vi should not be run until after the Vitiator sequence has been engaged.
6. Turn ON BNC Cabinet Power Strip.
7. OPEN Main Air (HP Air Tank Valve)
    a. Blue hand valve should be opened slowly as not to shock the lines
8. OPEN Air valve for the noise suppression system.
9. Ensure Shop Air in Test Cell #1 is CLOSED
10. Enter Test Cell #2 and OPEN all the supply gas bottles that are going to be used
11. Turn ON 24 VDC power supply for Test Cell #2 TESCOM Control Power.
12. OPEN Shop Air and Purge Air (High Pressure Air)

13. OPEN water supply for the Noise suppression system.
14. If required, set up any visual data recording equipment.
15. Evacuate all non-essential personnel to the control room
16. SET Initiator Fuel Regulator.
17. Turn ON Kissler Amplifiers
    a. Ensure they have been reset
    b. Check Gain for each channel
18. Connect Vitiator Spark Plug (if being used).
19. Connect the Engine Spark Plug.
20. Turn ON 24 VDC and 110 VAC in the control room cabinet

Running the Engine

1. Twist Emergency Stop Button clockwise (TEST CELL IS NOW LIVE)
2. Set All Engine Control Parameters (on BNC Pulse Generator)
    a. Send Engine Parameters to BNC
3. Set Main Air, Secondary/Purge Air, and all other gases pressures (ER3000) ON SAVAGE
    a. Set Main Air and Purge Air (ER3000)
        i. 001 Main Air
        ii. 004 Secondary Air
    b. Supply Gases in Test Cell #2 TESCOM Node Address
        i. 020 Main Fuel
        ii. 021 O2
        iii. 022 H2
4. Run the Control VI.
5. Enable the Test Cell on the VI.
6. OPEN required ball valves.
7. Verify Golf Course is clear
8. Sound the Siren
9. When area is clear, START record VCRs
10. Enable MSD Ignition switch
11. Manually engage Main Air flow

**********WARNING**********

The next step will result in the commencement of a run profile and ignition.

* Note: The 3-Way Ball Valve has a control in the Vitiator sequence. If the Vitiator is used then the 3-Way Ball will not divert through the engine until 375º F and will dump overboard at the end of the run at 175º F.

12. COMMENCE RUN
    a. High Speed DAQ will be triggered and the engine profile will commence
13. STOP RUN.
    a. Pulse generation will be stopped.
14. Push Emergency Stop Button IN
15. Secure MSD Ignition System
16. Stop Main Air Flow

17. If personnel are entering Test Cell, Push Emergency Stop Button IN
18. Secure 24VDC due to power flux in capacitor!

Test Cell #2
Standard Operating Procedures (S.O.P)
Engine Shut DOWN
(last modification date 01 December 2004)

1. Secure MSD Ignition System
2. Set Main Air and High Pressure Air to Zero on SAVAGE.
3. Vent all supply gases to ZERO
4. Ensure all BV have been closed on the NI control panel
    a. 3 Way Ball Valve, Purge, and Supply Gasses
5. Stop and Exit Control Code (ensure all relays have been set in original position)
6. Turn OFF Power Strip in BNC Timing Cabinet
7. Turn OFF 24 VDC and 110 VAC power supplies
8. Push Emergency Stop Button IN
9. Secure Main Air (HP Air valve in OFF position)
10. Secure Air for the Noise suppression system.
11. Remove Engine Spark Plug and Vitiator Spark Plug head
12. Close Shop Air, High Pressure Air, and Supply gases in Test Cell #2
13. Secure Kisslers
14. Secure water for the Noise Suppression system.
15. Secure TESCOM 24VDC power in Test Cell #2.
16. Stow Cameras and other equipment used in testing.
17. Turn OFF Warning Lights.
18. Close Test Cell #2.

APPENDIX C THRUST CALIBRATION

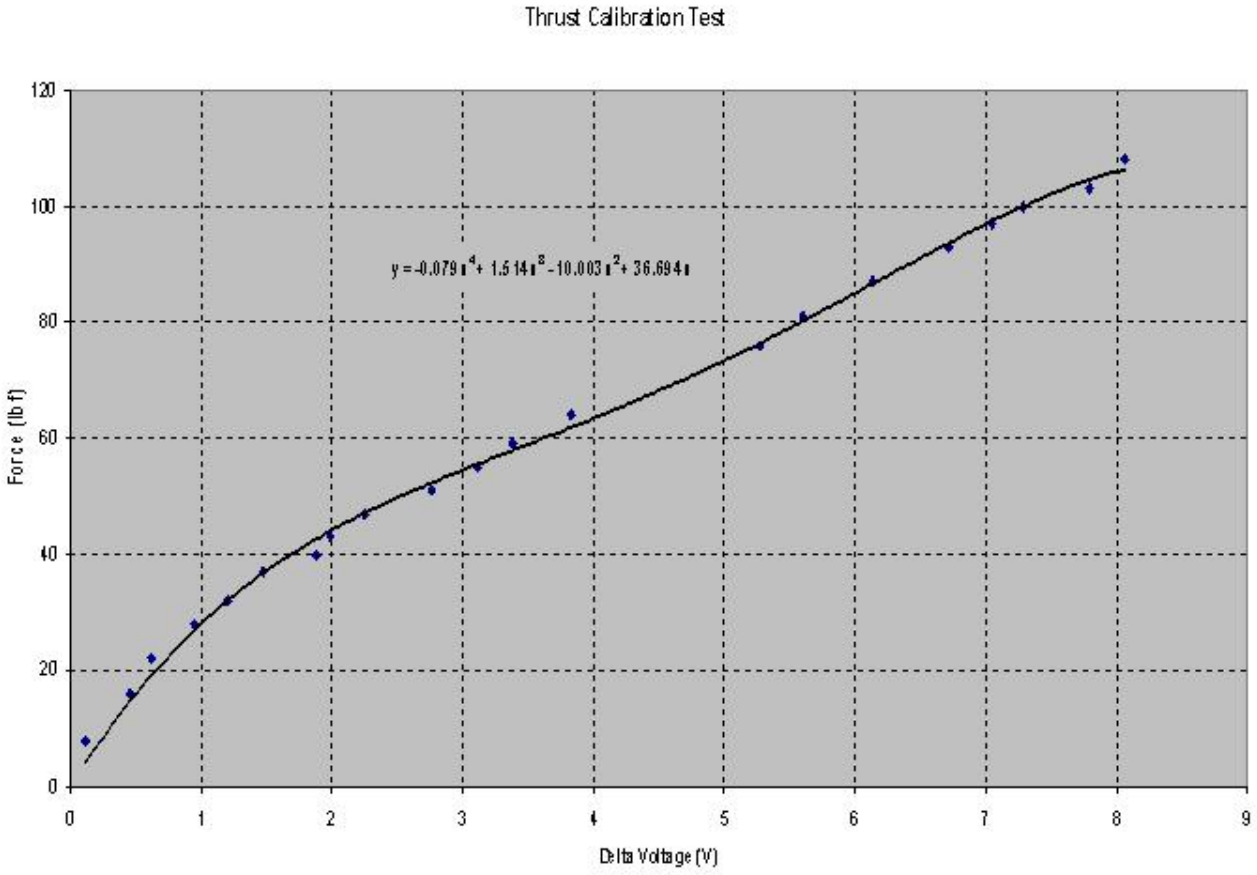

Figure 29. Thrust Calibration Curve Relating Displacement (ΔVoltage) to Force.

THIS PAGE INTENTIONALLY LEFT BLANK

APPENDIX D LABVIEW BLOCK DIAGRAMS

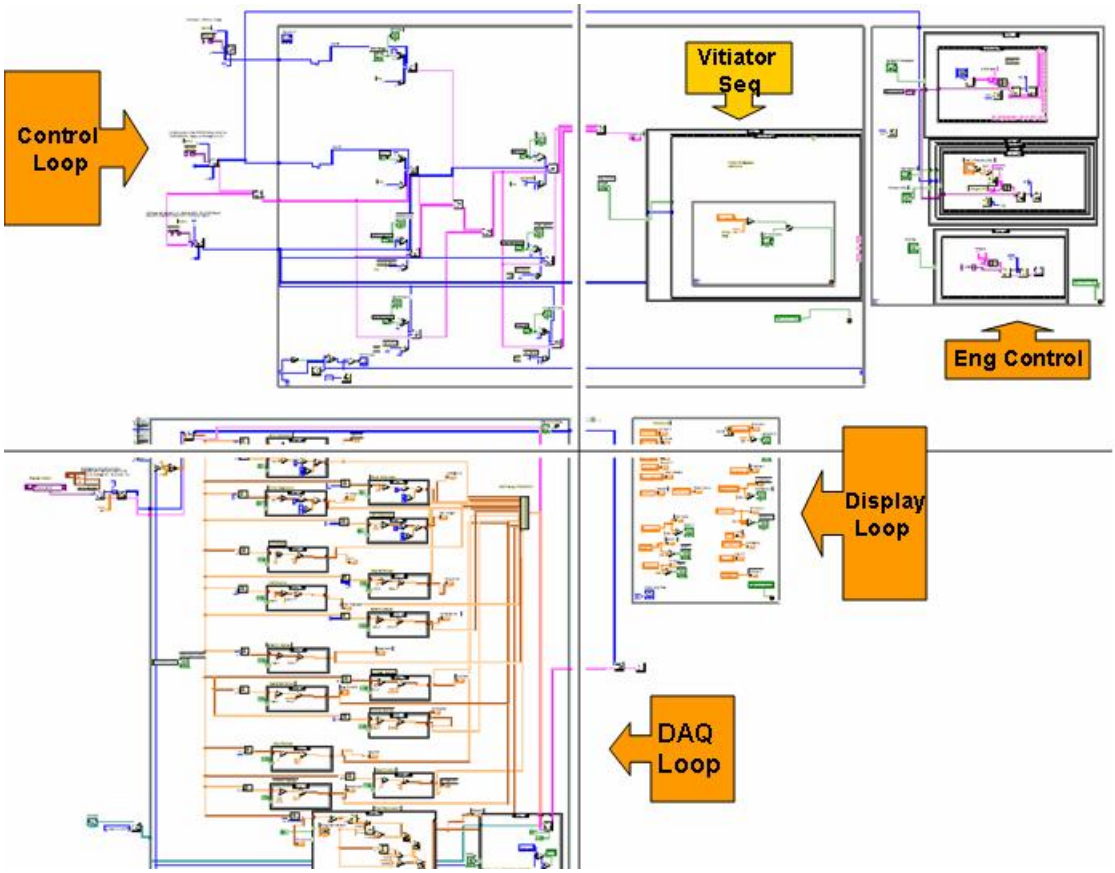

Figure 30. LabVIEW Control Loop Block Diagram

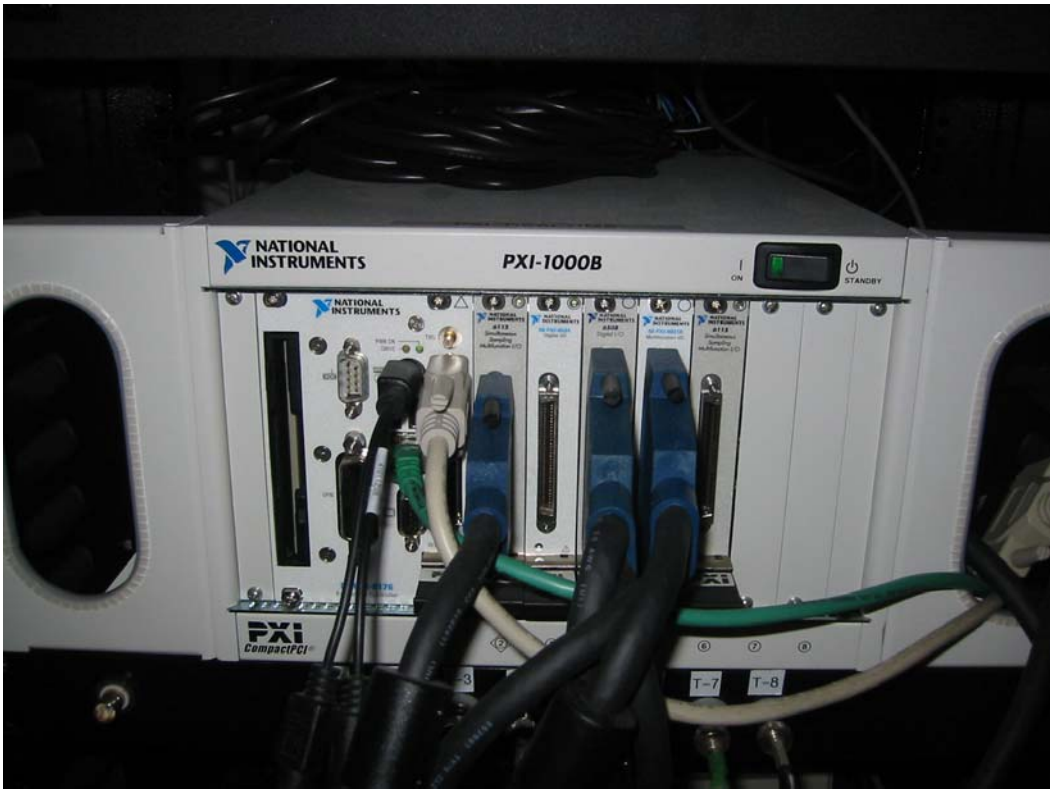

Figure 31. National Instruments PXI 1000B Instrumentation Chassis

Figure 32. Breakout Panels for PXI 6508 and PXI 6031E Data Acquisition Boards

APPENDIX E ENGINEERING DRAWINGS

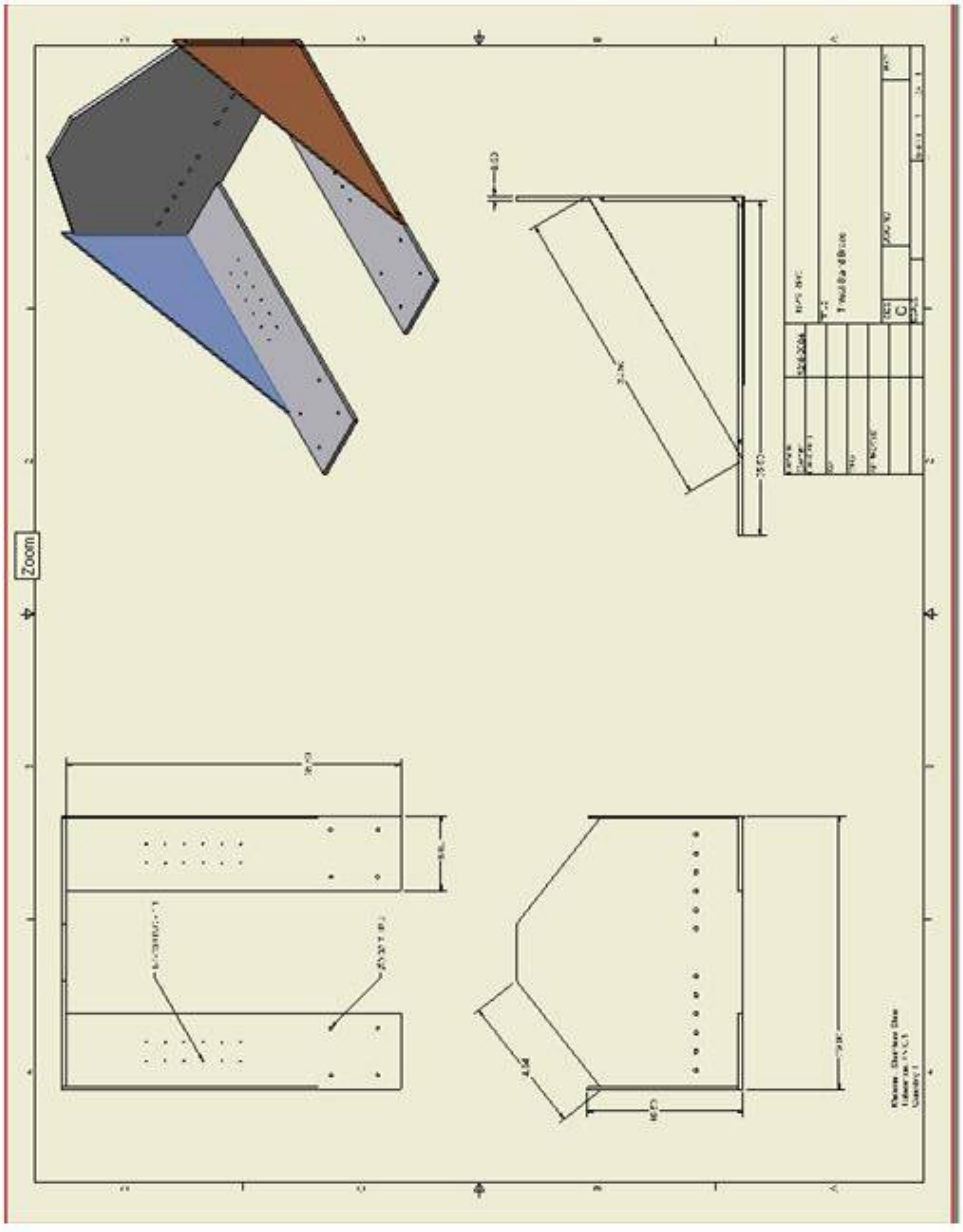

Figure 33. Thrust Stand Brace

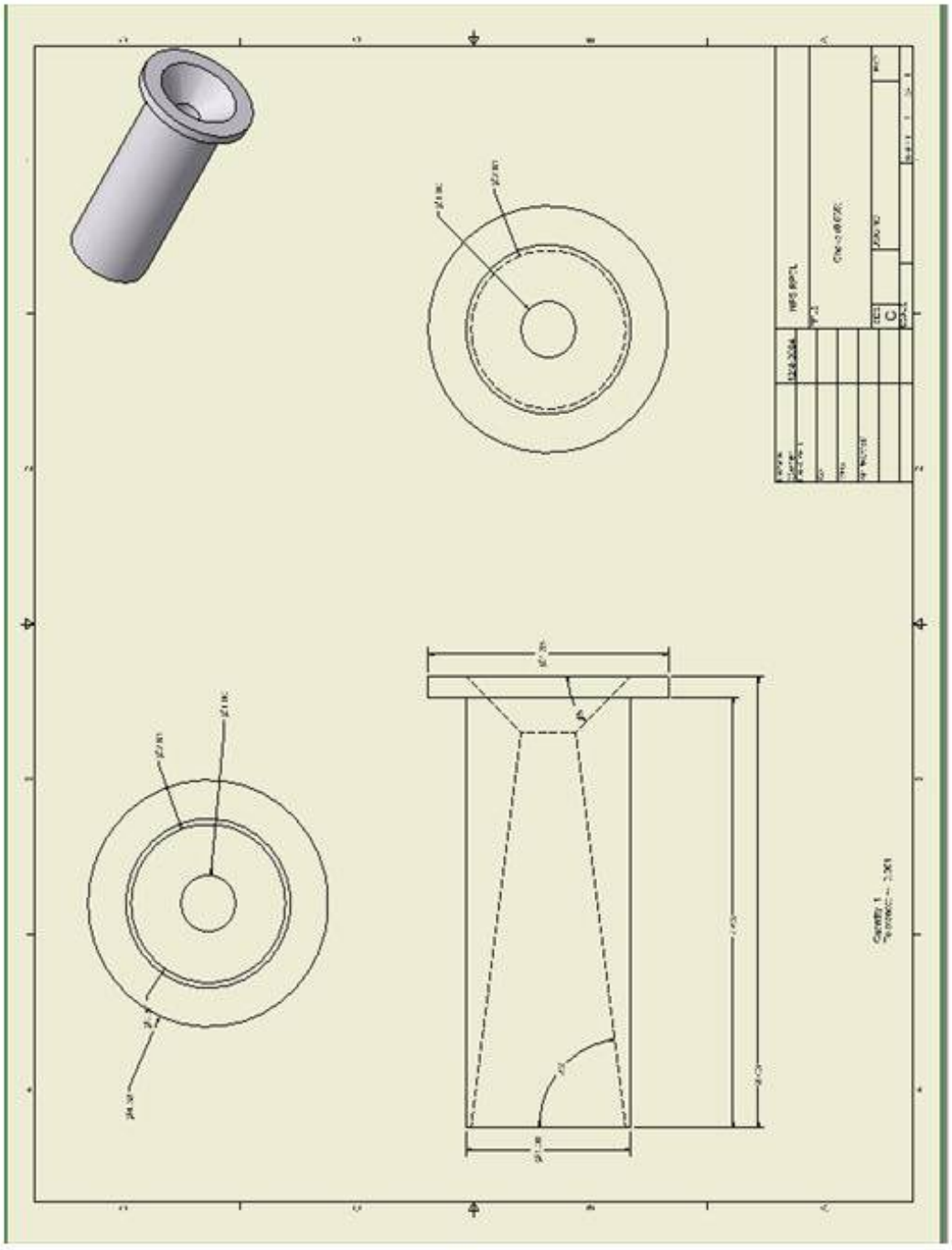

Figure 34. Main Air Choke (0.016637 m)

LIST OF REFERENCES

1) Brophy, C.M., Werner, S.P., Sinibaldi, J.O., Netzer, D.W., "Experimental Performance of a Valveless Pulse Detonation Engine," 51st JANNAF Propulsion Conference, Lake Buena Vista, Florida, November 18-21,2002.

2) Kuo, K., "Principles of Combustion" John Wiley and Sons, 1986, pp 230-282.

3) Werner, S., "Initiator Diffraction Limits for Pulse Detonation Engine Operation." Master's Thesis, Naval Postgraduate School, Monterey, California, December 2002.

4) Bussing, T., Pappas G., "An Introduction to Pulse Detonation Engines," 33rd AIAA Aerospace Sciences Meeting & Exhibit, Reno, Nevada, January 11-14, 1999, Paper No. AIAA 94-0263.

5) Forster, D., "Evaluation of a Liquid-Fueled Pulse Detonation Engine Combustor," Master's Thesis, Naval Postgraduate School, Monterey, California, December 1998.

6) Johnson, R., "Design, Characterization, and Performance of a Valveless Pulse Detonation Cycle," Master's Thesis, Naval Postgraduate School, Monterey, California, June 2000.

7) Robinson, J.P., "Influence of Ignition Energy, Ignition Location, and Stochiometry on the Deflagration to Detonation Distance in a Pulse Detonation Engine." Master's Thesis, Naval Postgraduate School, Monterey, California, June 2000.

8)Mattison, D., Brophy, C.M., Sander, S., Ma, L., Hinckley, K., Jeffries, J., and Hanson, R.K., "Pulse Detonation Engine Characterization and Control Using Tunable Diode-Laser Sensors," Journal of Propulsion and Power, Vol.19, No.4.

THIS PAGE INTENTIONALLY LEFT BLANK

BIBLIOGRAPHY

1) Brophy, C.M., Sinibaldi, D.W., Netzer, D.W., Johnson, R.G., "Operation of a JP-10/Air Pulse Detonation Engine," 36th AIAA/ASME/SAE/ASEE Joint Propulsion Conference, 17-19 July 2000, Paper No. AIAA 2000-3591.

2) Brophy, C., Werner, S., Sinibaldi, J. "Performance Characterization of a Valveless Pulse Detonation Engine," 41st Aerospace Sciences Meeting and Exhibit, Reno, Nevada, 6-9 January 2003, Paper No. AIAA 2003-1344.

3) Bussing, T., Bratkovich, T., Hinkey, J., "Practical Implementation of Pulse Detonation Engines," 33rd AIAA/ASME/SAE/ASEE Joint Propulsion Conference and Exhibit, Seattle, WA, 6-9 July 1997, Paper No. 97-2748.

4) Bussing, T., Hinkey, J. Kayae, L., "Pulse Detonation Engine Preliminary Design Considerations," 30th AIAA/ASME/SAE/ASEE Joint Propulsion Conference, Indianapolis, IN, 27-29 June 1994, Paper No. 94-3220.

5) Bratkovich, E., Aarnio, M., Williams, J., " An Introduction to Pulse Detonation Rocket Engines (PDREs)," 33rd AIAA/ASME/SAE/ASEE Joint Propulsion Conference and Exhibit, Seattle, WA, 6-9 July 1997, Paper No. 97-2742.

6) Eidelman, S., Sharov, D., Book, D., "Aerothermodynamics of Pulse Detonation Engines," 36th AIAA/ASME/SAE/ASEE Joint Propulsion Conference and Exhibit, Huntsville, Alabama, 16-19 July 2000, Paper No. AIAA 2000-3892

7) Touse, E. "Transmission of Detonation Waves across a sudden expansion with varying mixture composition," Master's Thesis, Naval Postgraduate School, Monterey, California, December 2003.

8)Van Wingerden, K., Bjerketvedt,D.,Bakke,J., "Detonations in Pipes and in the Open," Christian Michelson Research , Bergen, Norway, November 1999.

THIS PAGE INTENTIONALLY LEFT BLANK

INITIAL DISTRIBUTION LIST

1. Defense Technical Information Center
   Ft. Belvoir, VA

2. Dudley Knox Library
   Naval Postgraduate School
   Monterey, CA

3. Dr. Christopher Brophy
   Naval Postgraduate School
   Monetery, CA

4. Dr. Garth Hobson
   Naval Postgraduate School
   Monetery, CA